High Temperature Corrosion and Abrasive Wear of Boiler Steels

JELENA PRISS

TUT
PRESS

TALLINN UNIVERSITY OF TECHNOLOGY
Faculty of Mechanical Engineering
Department of Thermal Engineering

Dissertation was accepted for the defence of the degree of Doctor of Philosophy in Engineering on May 9, 2014

Supervisors: Professor Ivan Klevtsov, Department of Thermal Engineering, Tallinn University of Technology.

Ph.D. Andrei Dedov, Department of Thermal Engineering, Tallinn University of Technology.

Opponents: Ph.D. Arkadi Zikin, Head of Laser Surface Engineering, NUTECH GmbH, Neumünster, Germany.

Ph.D. Heinrich Suik, VKG OIL AS, Senior Advisor.

Defence of the thesis: June 20, 2014

Declaration:
Hereby I declare that this doctoral thesis, my original investigation and achievement, submitted for the doctoral degree at Tallinn University of Technology has not been submitted for doctoral or equivalent academic degree.

/Jelena Priss/

Katlateraste kõrgtemperatuurse korrosiooni- ja kulumisuuringud

JELENA PRISS

TTÜ
KIRJASTUS

Contents

Abbreviations and Symbols

AC^{2}T	Austrian Centre of Competence for Tribology
CFB	Circulating Fluidized Bed
DTE	Department of Thermal Engineering
EC	Erosion–Corrosion
EDX	Energy Dispersive X–ray
EO	Erosion–Oxidation
HHT	Hot Hardness Test
HT	High Temperature
HTC	High Temperature Corrosion
HT–CIA	High Temperature Cyclic Impact–Abrasion
HTE	High Temperature Erosion
LHV	Low Heating Value
LTC	Low Temperature Corrosion
NPP	Narva Power Plant
OM	Optical Microscopy
PF	Pulverized firing
SEM	Scanning Electron Microscopy
TUT	Tallinn University of Technology
Vol. %	Volumetric percentage
Wt. %	Weight percentage

Introduction

Wear in its various modes is the most important issue in many industrial applications. Correct steel selection could allow to increase the durability and operating reliability of components in boilers.

Combustion of Estonian oil shale containing inorganic matter produces several chemically active compounds leading to both fouling and accelerated high temperature corrosion of heating surfaces. The research of high temperature corrosion of different new steels in order to reveal the most corrosive–resistant and most suitable one for operation in the conditions of high temperature corrosion under influence of oil shale ash deposits is always of high importance. The ability to predict accurately the remaining life of the heating surfaces tubes subjected to intensive corrosion would help to reduce expenses of tubes replacement.

This study focuses on the relations between the properties of low and high alloyed steels and their corrosion and wear behaviour.

The Main Objectives of the Thesis:

- to study boiler steels durability in the conditions of corrosion, erosion and impact–abrasion at high temperatures;
- to rank tested steel grades according to their resistance to corrosion;
- to obtain data for analysis of the applicability of investigated steels for manufacturing of different components of boiler on the basis of carried out tests results.

Scientific Novelty

Scientific novelty of the doctoral thesis includes:

- New data of four boiler steel grades resistance to high temperature corrosion and abrasive wear have been obtained.
- New methodology of high temperature corrosion (HTC) testing has been proposed and realised in newly developed HTC tester.

List of Publications:

[PAPER-I]   **Priss J.**, Rojacz H., Klevtsov I., Dedov A., Winkelmann H., Badisch E. High temperature corrosion of boiler steels in hydrochloric atmosphere under oil shale ashes. *Corrosion Science*, 2014, 82, pp. 36–44. DOI: http://dx.doi.org/10.1016/j.corsci.2013.12.016

[PAPER-II] **Priss J.**, Klevtsov I., Dedov A., Antonov M., Rojacz H., Badisch E. High temperature cyclic impact/abrasion testing of boiler steels. *Key Engineering Materials*, 2014, 604, pp. 289–292. DOI: 10.4028/www.scientific.net/KEM.604.289

[PAPER-III]   Antonov M., Veinthal R., Huttunen-Saarivirta E., Hussainova I., Vallikivi A., Lelis M., **Priss J**. Effect of oxidation on erosive wear behaviour of boiler steels. *Tribo-Corrosion*, 2013, 68, pp. 35–44.Elsevier.DOI:http://dx.doi.org/10.1016/j.triboint.2012.09.011

Other publications (not included in the thesis):

[PAPER-IV]   J.Priss, I.Klevtsov. Strength calculations of slurry disposal pipeline. *The 22nd DAAAM World Symposium.* 23-26th November 2011, Austria Center Vienna, Vienna, Austria, pp. 1175–1176.
[PAPER-V]   Priss J., Klevtsov I., Dedov A., Antonov M. Investigation of boiler materials in respect to corrosion and wear. *"Proceedings of the 9th DAAAM Baltic Conference"* 24–26th April 2014, Tallinn, Estonia.

Author's Own Contribution

This section describes the author's contribution to the papers included in the thesis.

[PAPER-I]   I am the main author of the paper, responsible for the performance of tests, analysis of results, drawing the conclusions, literature review and data collection and had a major role in writing the paper.

[PAPER-II]   I am the main author of the paper, responsible for the performance of tests, analysis of results, drawing the conclusions, literature review and data collection and had a major role in writing the paper.

[PAPER-III] I took part in the analysis of results.

[PAPER-IV]   I am the main author of the paper, responsible for the analysis of results, drawing the conclusions, literature review and data collection and had a major role in writing the paper.

[PAPER-V]   I am the main author of the paper, responsible for the analysis of results, drawing the conclusions, literature review and data collection and had a major role in writing the paper.

Approbation:

Presentations at different international conferences:

- 22nd DAAAM World Symposium, 23–26th November 2011, Austria Center Vienna, Vienna, Austria;
- 23rd International DAAAM Symposium in 2012 in Zadar, Croatia;
- 22nd International Baltic Conference of Engineering Materials, Tribology-BALTMATTRIB 2013 in Riga, Latvia;
- 9th DAAAM Baltic Conference" 24–26th April 2014, Tallinn, Estonia.

1   REVIEW OF THE LITERATURE

1.1   Fundamental mechanisms of wear

The wear is usually defined as the process of material removing from the surface due to interaction with tribological elements. The most typical mechanisms of wear are presented in Figure 1.1.
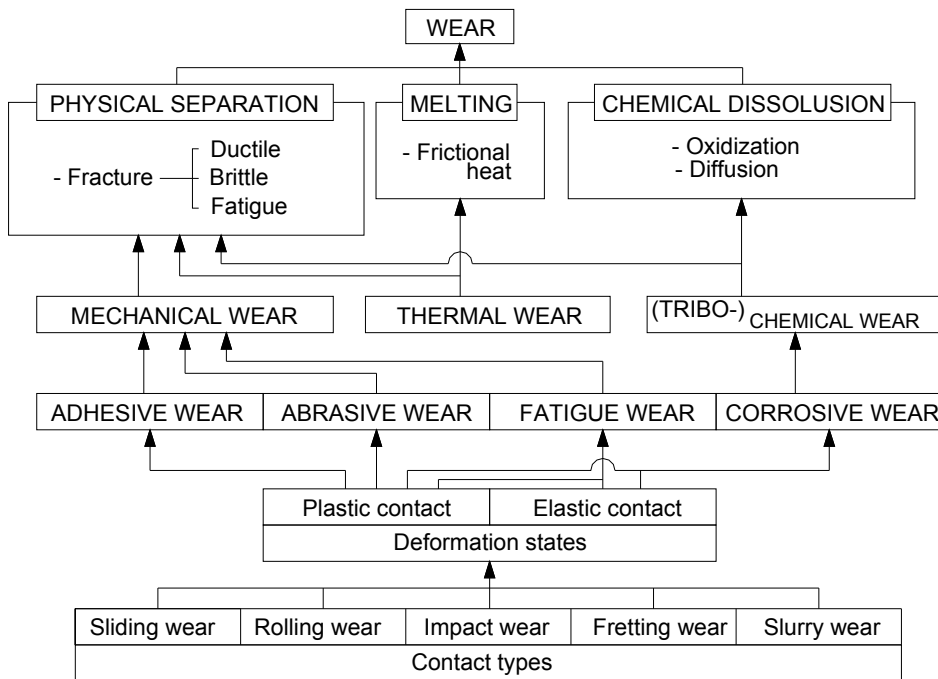
Figure 1.1. Wear classification.

In present research abrasive wear of boiler steels were investigated.

Corrosion, corrosive wear and oxide formation at high temperatures

The corrosion of the metal is spontaneous process between the metal and its surrounding environment, during which damage and destroy of the material happens.

Material removing from the surface due to interaction with tribological elements in corrosive media, the resultant wear is called corrosive wear. The most dominant corrosive element in air is oxygen and wear in air is called oxidative wear [1].

Typical materials for power plant components are ferritic or austenitic heat resistance steels or super alloys that show oxidation resistance at high temperatures (500–800 °C) [1].

Alloyed steel changes the picture of the oxide formation, especially since chromium and nickel in the steel will be involved in the oxidation.

Figure 1.2. presents a schematic view of the oxidation of a metal surface. The diffusion depends on the metal/alloy type, temperature and the atmospheric conditions [1].
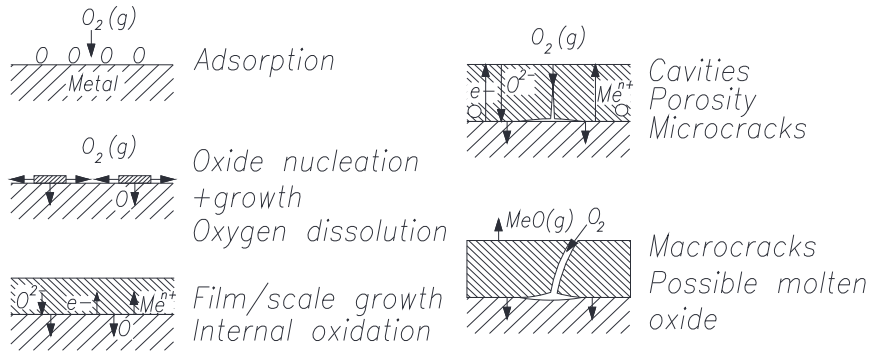
Figure 1.2. Schematic illustration of main steps and chemical formulation of metal-oxygen reactions [1].

The reaction between a metal and oxygen may be represented by the following equation [1]:

$$aM + (b/2)O_2 = M_aO_b,$$ (1.1)

where M – oxidizable metal;
         O – oxygen;
         a, b – stoichiometric coefficients.

As the result of oxide formation, many possible ways of boiler metal wear exist. Firstly, it is a high– and low–temperature corrosion (HTC/LTC), when formed oxide scales influence the thermal transfer in boiler.

Many parameters determine the course of high–temperature corrosion [2]. It is influenced mainly by the structure and stability of the oxide layer on the metal. External forces like cleaning cycles, thermal stresses, that factors result damage to the oxide layer on the tube metal.

Erosive wear

Erosive wear is loss of material from a solid surface due to relative motion.

Material loss due to erosion is measured as the ratio of the mass of removed material with respect to the mass of erosive particles. Illustration of the erosive wear is shown in Figure 1.3. Mechanisms of erosion can involve both plastic deformation and brittle fracture [3].
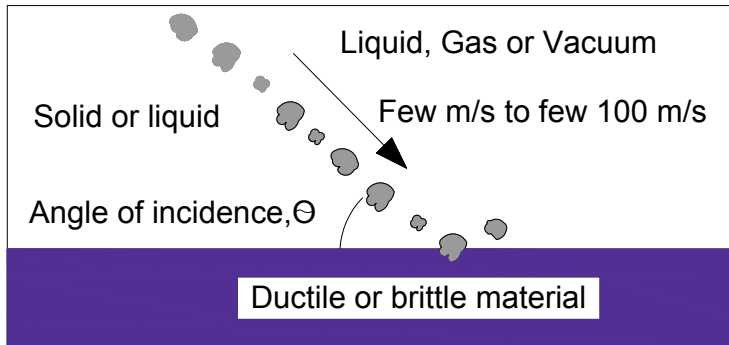
Figure 1.3. Explanation of erosive wear [3].

H. Uuemõis and I. Kleis [4] has found a number of parameters influence erosion: impact velocity, impact angle, particle size, particle concentration, hardness ratio of the abrasive and the material subjected to wear, geometry of abrasive particles, strength of abrasive particles, test temperature, corrosiveness of environment, content of additives in the abrasive (fluid or solid).

The most important parameter of erosion is impact angle. The maximum wear rate of ductile materials is at an impact angle between 30° and 60°, while the maximum wear rate of brittle materials occurs approximately at the impact angle of 90° [5].

Abrasion

Abrasion is the most common form of wear in industry. It is defined as: "the wearing away of any part of a material by frictional action of hard particles through the surface of a softer material" [6].

When one surface (usually harder than the second) cuts material away from the second, two body abrasion occurs. This mechanism very often changes to three body abrasion as the wear debris then acts as an abrasive between the two surfaces. Explanation of abrasion is presented in Figure 1.4 [3].
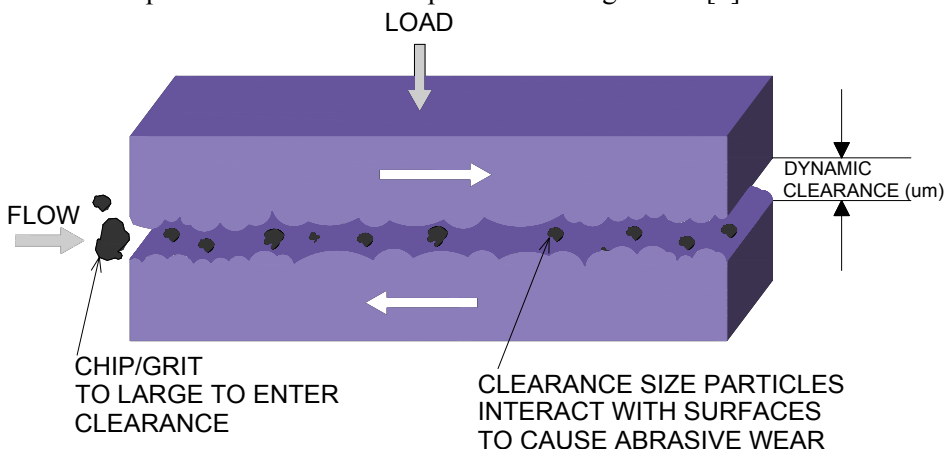
Figure 1.4. Explanation of abrasion [3].

1.2 Modes of wear in boilers

Gas – side processes in boilers

According to A. Ots [2] the purpose of a boiler is to transfer the energy released during fuel combustion (expressed by flue gas temperature) to flue gas and, thereafter, to the medium to be heated. The latter is usually water, steam, or air. For gas–side processes, the main equipment in a boiler is a heat exchange surface. Gas-side processes in a boiler represent a set of interrelated and consecutive chemical and physical phenomena, which ultimately determine the rate of heat transfer from flue gas to the heated medium, the lifetime of the boiler tubes, and the design and arrangement of the heated exchange surfaces. The nature of gas–side processes is determined by fuel properties and combustion technology.

The typical conditions of fire side corrosion of tubes of power plant steam boiler heating surfaces are presented in Figure 1.5.
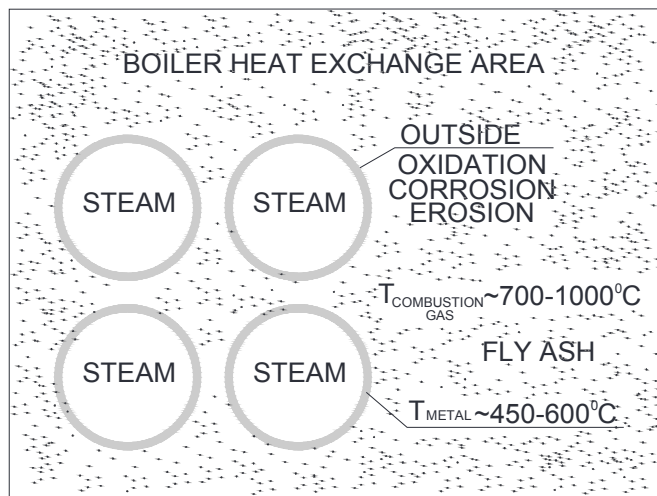
Figure 1.5. Fireside corrosion and wear.

Conditions in fluidized–bed boilers (e.g., elevated temperatures, oxidizing atmospheres and impacts by fluidized sand and ash particles) may cause significant wearing of some boiler components, such as heat exchanger tubes, by a combination of oxidative attack and erosive wear [2, 7, 8].

M. Antonov [9] describes that erosion–corrosion is a result of material wastage rates in power generation industry. Boiler components, such as superheater and reheater in fluidized bed boilers are suffering from fly-ash erosion. Major constitutes of the fly–ash are SiO_2, Al_2O_3, and Fe_2O_3. To reduce the wear rates there is imposed limits for the flue gas velocities (12–13 ms^{-1} for erosive ash having high silica content and 18–20 ms^{-1} for less–erosive ash), but also boiler efficiency should be considered.

Wear problems in circulating fluidized bed boilers

Oil shale is a sedimentary rock containing organic matter [2] and the main source in Estonia. Around 90 % of the electricity in the country is produced from oil shale at the Narva Power Plants (NPP). The lower heating value (LHV) of oil shale used for electricity production is 8.3–8.4 MJ/kg [10].

Oil shale is characterized as a fuel with a high content of alkali metals and chlorine. Burning that kind of low–grade fuel is associated with several problems: dissociation of carbonate minerals, high CO_2 emission levels, ash handling and storing [2].

For minimizing the environmental impact of power production, the application of modern Circulating Fluidized Bed (CFB) technology at the NPP (Figure 1.6) provides advantages in utilization of upgraded oil shale with the LHV at up to 11.0 MJ/kg [10]. CFB of solid fuels, a technology that is still in the development stage, is the newest trend in thermal power plants [2].

In CFB combustion boiler, the inert bed material is in the fast fluidization mode. Particles move upward (ash particles by burning of oil shale), get separated there and return to the bottom of the furnace. A circulating contour is created [2].

Scheme of CFB boiler in NPP is presented in Figure 1.6 [11]. The potential problems of HTC, LTC and erosion in NPP CFB boiler parts are summarized at Table 1.1.
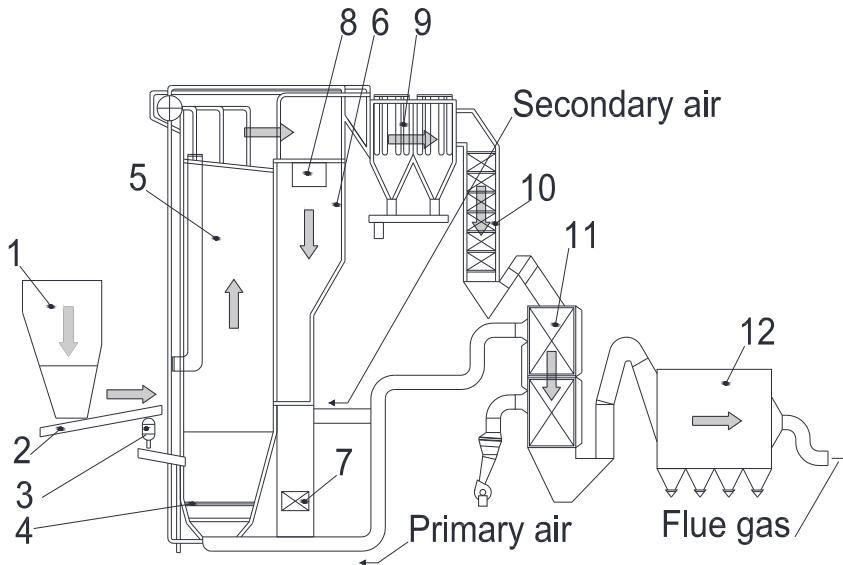
Figure 1.6. Scheme of oil shale- fired CFB boiler [11]: 1 – Raw fuel silo, 2 – Fuel feeder, 3 – Secondary fuel crusher, 4 – Grate, 5 – Furnace chamber, 6 – Separating chamber, 7 – Fluidized bed internal heat exchange (Intrex), 8 – Separator of solids, 9 – Convective superheater and reheater, 10 – Economizer, 11 – Air preheater, 12 – Electrical precipitator.

Table 1.1. NPP CFB boiler components potential wear [2, 8, 12].

Posi-tion	Potential wear			
	Surface	HTC	LTC	Erosion
2	Fuel supply system (plates)			X
4	Furnace chamber	X		X
5	Separating chamber	X		X
7	Fluidized bed internal heat exchanger	X		
9	Convective superheater and reheater	X		
11	Air preheater (APH)		X	
10	Economizer	X	X	X
7	Intrex Superheater III	X		X
7	Header; inlet			
7	Header; outlet			
7	Reheater	X		X

1.3 Corrosion of boiler tubes and waste incineration systems

Gas-side corrosion

According to A. Ots [2] "Gas-side" corrosion develops in an environment defined by the interaction of flue gas with the ash deposits found on the boiler tube surfaces. In boiler design, it is customary to divide the flue gas corrosion processes into those taking place at low and high temperatures, noting the differences in the course of these processes. Low-temperature corrosion is linked to the condensation of sulphuric acid and/or water vapour from the flue gas onto the heat transfer surface. High-temperature corrosion develops at higher temperatures than during the low-temperature processes, but there is no definite temperature limit.

Formation of aggressive chlorides and sulphur dioxides in flue gases in industrial boilers is the result of incineration of biomass and waste [13]. Table 1.2 presented the number of surface phenomena in waste incineration systems.

According to J. Adamiec [13] research corrosion processes in the combustion chamber of waste incineration systems have an oxidizing nature, connected with the presence of nitric and chromium acids, iron and copper salts, nitrites, chromates, sulphuric, hydrochloric and phosphoric acids, organic acids, solution of alkaline salts and halides. As the result, the presence of a mixture of the above mentioned compounds and increased temperature may lead, among others, to crevice or pitting corrosion.

Table 1.2. Typical surface phenomena in waste incineration systems [13].

Corrosion processes connected with the presence of humidity	Corrosion processes as a result of increased temperature
- Surface corrosion	- Sulfiding
- Crevice corrosion	- Carbonizaton
- Stationary pitting corrosion	- Formation of metal-dusted areas (dusting)
- Stress corrosion	- Nitriding
- Intercrystalline corrosion	- Sulfiding

The influence of oil shale ash on metal corrosion
According to A. Ots investigation [2] in oil shale boilers, in addition to the very heavy coverage of heat transfer surfaces by ash deposits, another important problem occurs: the high-temperature corrosion of the same boiler tubes. This corrosion is quite acute for the super heater metal. Corrosion-activating components form during the process of fuel (oil shale) properties but also to the combustion technology.

There have been studied [14] the impact of oil shale ash deposits on tubes made from the steels rich in nickel (Ni – 12.16 %, Cr – 16.03 %) and tubes covered with coatings (Ni – 73 %, Cr – 21 %, Ni/Cr – 1.5). The results clearly demonstrate the influence of the steel composition on the corrosion rate. A more detailed investigation of the corrosion rate factor of austenitic steels demonstrated that its value correlates well with the ratio Ni/Cr in metal. This can be seen on Figure 1.7, where the influence of the ratio Ni/Cr on the corrosion rate factor of austenitic steels is presented.
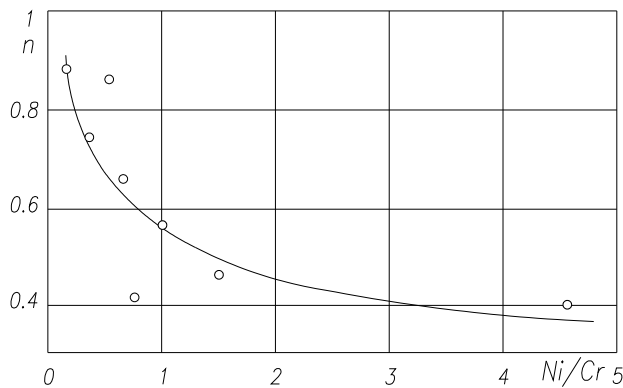
Figure 1.7. Influence of the ratio Ni/Cr on the corrosion rate factor during the corrosion of austenitic steels under the impact of a stable oil shale ash deposits at 580 °C [14].

The figure illustrates that the value of *n* decreases under the impact of a chlorine-containing deposit with a decrease in the chromium content or in the Ni/Cr ratio of the metal. Therefore, the superheater tubes of an oil shale boiler are more resistant to corrosion when made of a steel in which the ratio Ni/Cr exceeds 1 [14].

High temperature corrosion in the presents of chlorine
A. Ots [2] describes, that an important factor in alloy corrosion can be the reaction between the oxides formed from the different alloy components. As a result of these reactions, a stable composite oxide, with completely new characteristics and with a diffusion-resistant intricate structure, may form on the alloy surface. Depending on the alloy composition and on the external parameters, a composite-oxide might include not all, but only a certain number, of the alloy components. The diffusion rate of the reacting components in this type of composite composition oxide layer is generally much slower than in a pure metal oxide. These types of oxides are found in corrosion-resistant alloys.
High-temperature corrosion in an atmosphere containing chlorine is complex. It leads to the formation of scale with an exemplary structure presented in Figure 1.8 [15]. This illustration was derived according to Y. Kawahara [15] analyses of corrosion products and thermodynamic consideration.
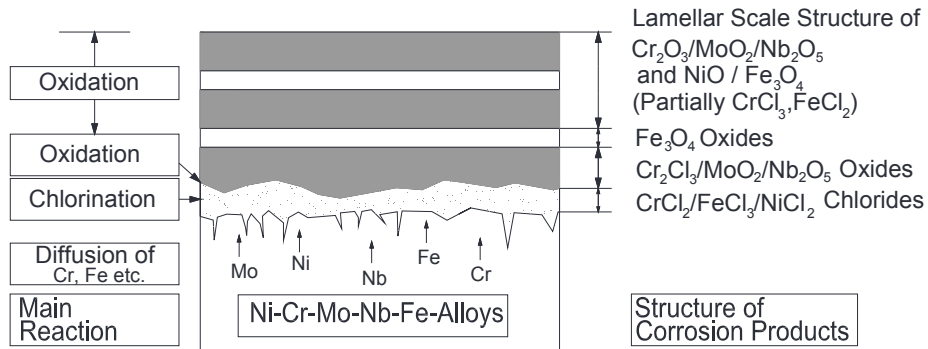
Figure 1.8. Structure of scale formed in Ni-Cr-Mo-(Nb, Fe) alloy as a result of high-temperature chlorine corrosion [15].

1.4   Erosive – corrosive processes in boilers

Erosion-oxidation and erosion–corrosion mapping
There are a number of factors which were mentioned before [4] that influence the erosion–oxidation (EO) of the materials, one of them is the oxidation kinetics, which is affected by the temperature and the alloy [5] and should be considered as well.
The erosion–oxidation process is divided into different regimes [5], ranging from pure erosion to pure oxidation.
Laboratory testing seemed to indicate erosion, erosion–corrosion and pure corrosion processes according to weight loss and temperature increase [5].

Figure 1.9 illustrated the increasing of wear rates with an increase in temperature to some peak and then decrease with a further increase in temperature.
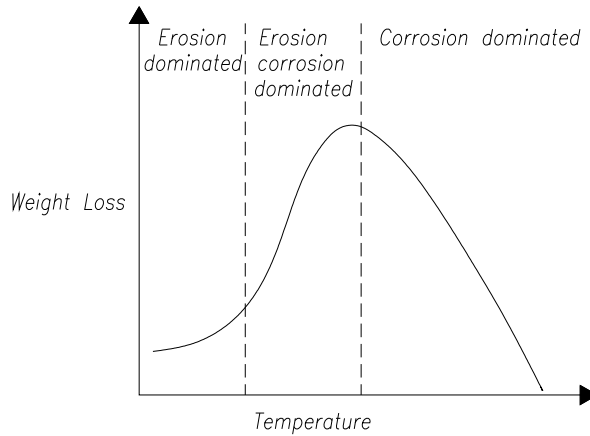
Figure 1.9. Diagram showing the erosion–corrosion response of metals to temperature changes [16].

Erosion–oxidation mapping (EO maps) and more recently erosion–corrosion (EC maps) is a popular way [17] to represent the system behavior under different EO and EC conditions. This is the best option to select the material, to understand of materials response under wide ranges of conditions [18].
EO maps are useful to determine what will happen when conditions change. Figure 1.10 represent the example of EO map.
More recently, such mapping has been further developed into modelling of materials selection maps [19]. Figure 1.11 represent the example of such mapping.
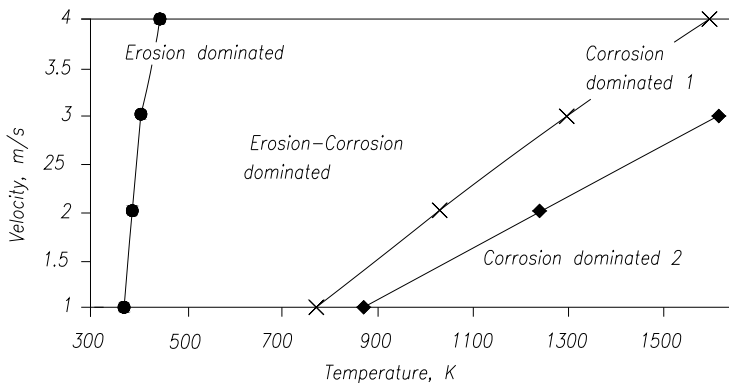
Figure 1.10. EO map evaluated by Stack's simulation program [20].
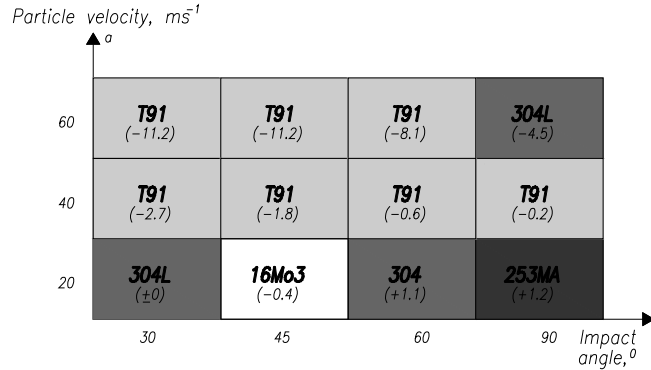
Figure 1.11. Materials selection map, using the lowest average wear loss (the lowest weight loss/the highest weight gain) as a selection criterion, with (+) indicated mass gain and with (−)indicated mass loss for selected materials [19].

Erosion processes in boilers

The wear of boiler's heat transfer surface consists of the thinning of the tube wall over time [2]. Hard particles, either directly from the fuel or from the ash that forms after combustion, can cause erosive damage to boiler components [21].

According to A. Ots [2] the increase in diffusion resistance of the oxide layer over time is a significant factor in the boiler tube corrosion process. Therefore, any damage to the oxide layer on the boiler tubes and other similar phenomena that reduce the diffusion resistance of the oxide layer will accelerate the rate of metal corrosion. For example, fly ash erosion refers to damage caused by ash particulate entrained in high-speed flue gases striking metal surfaces [21].

A. Ots [2] declared, that the term, erosive wear, is used to define the wear of the material caused by a force acting periodically on a metal surface. If the erosive impact of the force on the metal damages the protective oxide layer, the process is defined as corrosive-erosive wear, and the periodic crumbling of the oxide layer on the metal surface accelerates the corrosion process.

Erosive damage can be attributed to a number of different sources, such as particles in fly ash [21], temperature fluctuations, falling slag and soot blowing.

The fact that erosion–oxidation problems still inconvenience power generation, for example, in fluidized–bed boilers, after a few decades of practical and theoretical experience, reflects that the phenomena are complicated [19].

Basic problems of abrasive impact wear

Wear caused by the abrasive impact wear action of hard particles [21] is dominant problem in many industrial processes. One of the wastage mechanisms is impingement of particles on the surface [22], which causes abrasive wear.

The abrasive wear theory assumes that abrasive particles leave a wear area of the same cross-sectional shape [6]. Specific mechanical and geometrical properties of abrasive particles which are getting in contact with the wearing surfaces could restrict the life time of costly machine parts [23].

Many researches are done to understand of the response of various materials exposed to this type of wear [24 – 25].

1.5   Research process

The investigation of problem existed in some boiler components could be prepared according to the scheme (Figure 1.12) proposed by M. Antonov [26].
Corrosion and wear investigation have two options for process determination. The first method is industrial testing and the second is laboratory testing.
The laboratory test is performed according to standards, usually involves test specimens and could be executed in short time [26].
The test samples are smaller than the real component and of simple geometry that makes the test more convenient and enables to raise the level of control of conditions and of tracking the tribosystem behaviour [26].
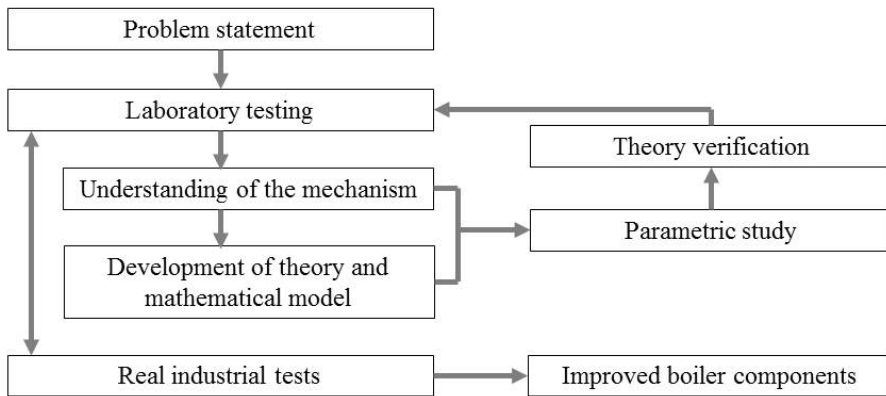
Figure 1.12. A schematic overview of the researching process to improve the performance of the boiler parts [26].

Tribotests

Tribology (from the Greek τριβος– rubbing or attrition) is defined as "the science and technology of interacting surfaces in relative motion" [3]. Tribotester is the machine or apparatus for simulation the wear in laboratory conditions.
Tribotests could be classified by rising of the degree of realism (how closely they imitate the conditions of real application) as laboratory test, simplified component, component, sub-system test [26]. The comparison between laboratory testing and industrial testing with more evaluation aspects is given in Table 1.3.

Table 1.3. Comparison between laboratory testing and industrial testing [26].

Criteria	Laboratory testing	Industrial testing
Degree of realism	Lower	Higher
Duration of the test	Several hours	Several months
Cost of the test	Lower	Higher
Level of the conditions control	Higher	Lower
Ability to study individual, isolated wear mechanisms	Higher	Lower

Laboratory tests of Department of Thermal Engineering

The corrosion tests of steels (X12CrNiTi18-9, X10CrMoVNb9-1) in laboratory of Department of Thermal Engineering (DTE) have been carried out in accordance with standard techniques [27, 28]. These tests have been performed in electrically heated vertical tube-type furnaces with an inner diameter of 40mm (Figure 1.13). The combustion products of natural gas have been directed into the furnaces by the pipe header. The combustion gas velocity in the furnaces has been 15–18 cm/s. In order to avoid condensation of water vapour the pipe header has been heated by electrical heating coils. The temperature in the furnaces has been maintained at 540 °C, 580 °C and 620 °C with accuracy ± 2 °C [29].

The corrosion tests have been performed on flat polished specimens with dimensions 3x10x40 mm, which have been cut from original boiler tubes. Prior to the tests all specimens were degreased, precisely measured and weighed. They were then coated with a mixture of oil shale ash and ethyl alcohol for imitation of oil shale on-tube deposits. Electrical precipitator ash, with chlorine content of about 0.5 %, was used in the laboratory experiments [29].
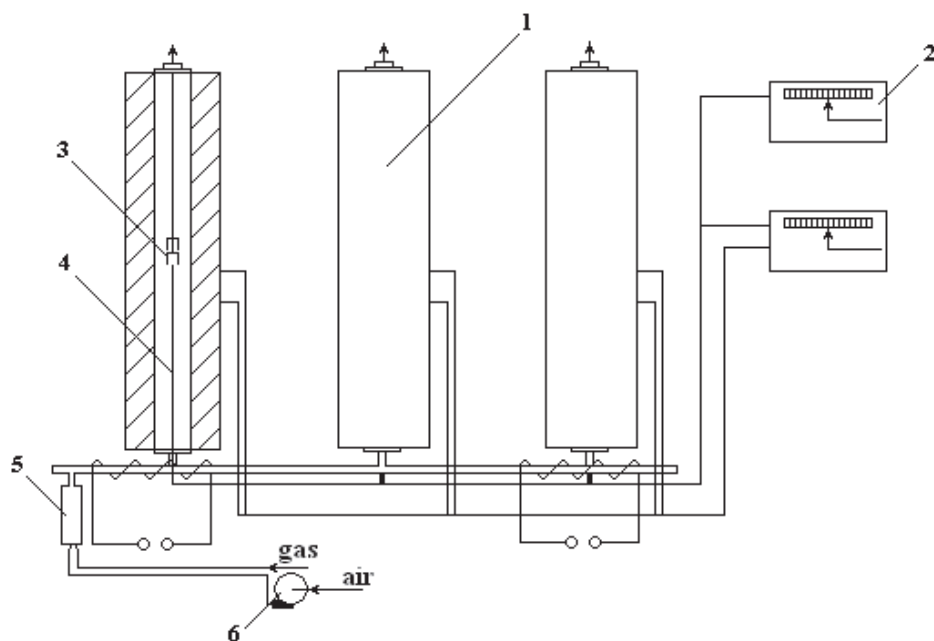
Figure 1.13. The scheme of laboratory tester for investigation of steels high temperature corrosion: 1 – electrical furnaces; 2 – tools for temperature measurement and control; 3 – test specimens; 4 – thermocouples; 5 – combustion chamber; 6 – fan [29].

The removal of corrosion and oxide scales from the post-test specimens was performed in the environment of liquid sodium by blowing ammonia [30]. The quantity of corroded material was determined as the difference of mass of clean specimens before and after testing. The accuracy of weighing was ± 0.1mg. On the basis of mass difference the corrosion depth was calculated ($\Delta S'$, mm):

$$\ln\Delta S = \alpha - \beta{\cdot}T^{-1} + (\gamma + \varepsilon{\cdot}T)\ln\tau, \qquad (1.2)$$

where ΔS – the corrosion depth [mm];

   τ – the test duration, [h];

   T – metal temperature, [K];

   α, β, ε and γ – coefficients which depend on the ash characteristics, the particular fuel, the steel grade and temperature of the metal.

The binomial term ($\gamma + \varepsilon{\cdot}T$) is usually defined as an exponent of the corrosion process [31–34].

Experiments

Typical materials for power plant components are ferritic, austenitic heat resistance steels or super alloys. For present research four high temperature resistance steels used at Narva Power Plants were investigated in the HTE, HTC and HT–CIA testers, Table 1.4. Additionally, HHT measurements at room and elevated temperatures were done for steels characterization. All samples for tests were cut from original boiler tubes in laboratory.

HTC, HTE and HT – CIA tests have been performed for better understanding steels behaviour under HT corrosion – abrasion conditions. All testers are accelerators and test conditions do not agree with real conditions in industrial boiler processes. The temperatures 500 and 600 °C for all tests were chosen for maximal simulation combustion gases temperature in boiler.

In HTC test oil shale ash were used for simulation deposits and pure HCl for getting maximal corrosion under such extreme conditions.

Erosion (HTE) at such a high speed (80 m/s) was selected to reduce possible role of oxidation during erosion-oxidation process. Erosion tests were conducted at impact angles of 30° and 90°, respectively.

HT-CIA test was done for investigation steels behaviour. Test conditions are extremely high and could not appear in boiler in the same type, but different variations of it could be found in fuel handling systems.

Table 1.4. Testing matrix.

Hot hardness test (HHT) Temperature range: RT, 100 – 800 °C	High temperature corrosion (HTC) test Temperature range: 500, 600 °C Conditions: HCl, oil shale ash
High temperature erosion (HTE) test Temperature range: 500, 600 °C Conditions: 80 m/s, 30°, 90°	High temperature cyclic impact abrasion (HT-CIA) test Temperature range: 500, 600 °C Conditions: 0.8 J, abrasive 3 g/s, 45°

1.6 Steels properties

The chemical compositions of all steels (Table 1.5) are given in Table 1.6 [PAPER I].

Table 1.5. Investigated steel grades

	Investigated steels		Equivalent steels	
	Steel Grade	Standard	Steel Grade	Standard
A	12X18H10T	ГОСТ 5632-72	X12CrNiTi18-9	DIN 17440
B	X10CrMoVNb9-1	EN 10216-2	P91	ASME SA-335
C	12X1МФ	ТУ14-3P-55	13CrMoV42	DIN 17155
D	TP347HFG	ASME SA-213	X8CrNiNb16-13	EN 10028-7

Table 1.6. Chemical composition of investigated steels in wt. % [PAPER I].

	Tested steel		Composition, wt. %								
	Steel Grade	Standard	Fe	C	Si	Mn	Cr	Ni	V	Mo	Others
A	12X18H10T	ГОСТ 5632-72	69.77	0.12	0.83	-	18.48	10.39	-	-	Ti=0.52
B	X10CrMoVNb9-1	EN 10216-2	89.09	0.12	0.40	-	8.86	-	0.37	1.08	Nb=0.21
C	12X1МФ	ТУ14-3P-55	95.1	0.15	0.46	1.01	1.44	0.39	0.38	1.23	Mo=1.23
D	TP347HFG	ASME SA-213	66.16	0.1	0.66	1.98	18.64	11.19	-	-	Nb=1.37

In order to avoid variant reading the steels grades in this thesis were designated according to DIN and EN standards.

Material A is an austenitic, corrosion-resistant steel X12CrNiTi18-9. This steel has a high temperature resistant microstructure Cr – 18 %, Ni – 10%, which improves the resistance against corrosion in reducing environments and stress corrosion cracking [35]. Additionally titanium is added (0.52 %) to stabilize the carbon and the chromium in the matrix and increasing the fracture toughness by precipitating intergranular TiC [36].

Martensitic steel B (X10CrMoVNb9-1) is a chromium alloyed high strength steel with increased creep resistance. At the chromium content of 9 % and the added molybdenum (1.08 %) the pitting and crevice corrosion resistance is increased [37, 38]. Steel C is a pearlitic steel 13CrMoV42 with a chromium content of 1.44 %.

The austenitic steel X8CrNiNb16-13 (D) has homogeneous structure in bimodal distribution of the grain size. In this steel Nb is added to increase the strength and the resistance against different corrosive attacks [39].

Metallographic cross sections of all investigated steels in AC^{2}T [PAPER I] can be seen in Figure 1.14. Steel A, as seen in Figure 1.14a reveals austenitic microstructure, with intergranular TiC-precipitations and TiN inclusions. In Figure 1.14b the martensitic steel B can be seen, revealing its typical microstructure. The pearlitic structure of 13CrMoV42 can be seen in Figure 1.14c. Steel D (Figure 1.14d) reveals austenitic structure with twin grain boundaries and intergranular precipitations (mostly NbC).

Figure 1.14. Microstructures of the investigated steels: (A) austenitic steel X12CrNiTi18-9, (B) martensitic steel X10CrMoVNb9-1, (C) pearlitic steel 13CrMoV42, (D) austenitic steel X8CrNiNb16-13 [PAPER I].

1.7   Hardness at room and elevated temperatures

Hardness is the resistance of a material to plastic deformation. The hardness is higher for material which is more difficult to plastically deform under load.

Hardness is one of the most important and easily measurable properties which has a major effect on abrasive wear. By abrasive wear, material wear rate depends on material hardness– if it is lower than abrasive hardness, microcutting of the surface may take place. If material hardness is higher than abrasive hardness, clear removal of the material usually does not take place and the entire process has the nature of fatigue [40].

The hardness test at room and elevated temperatures was done for steels investigated. The tests were performed in Austrian Centre of Competence for Tribology (AC^2T). Figure 1.15 displays the hot hardness tester.

The room temperature hardness was determined by standard Vickers hardness testing procedure. Average hardness values were calculated from 10 indents per specimen.

The hot hardness test (HHT) is based on the Vickers HV10 method extended for elevated temperature up to 800 °C. A load of 10 kg was chosen to measure the compound hardness of steels. As prevention against oxidation, the whole test is performed under low vacuum condition (5 mbar). Sample´s position can be set by an actuator and variation of hardness over temperature curves can be measured on one sample. Three indents at each temperature were done for statistical evaluation. The diagonals of the indent marks were measured by

means of optical microscopy after cooling down and Vickers hardness was calculated. Figure 1.16 presents example of HHT indents. For this investigation the hardness was measured at room temperature (RT), 100, 300, 500, 600, 700 and 800 °C, respectively [PAPER II].

Steels have an initial HV10 Vickers hardness of ~221 HV10 (A); 235 HV10 (B); 146 HV10 (C); 180 HV10 (D) at RT which is slowly declining with increasing the temperature, as seen in Figure 1.17 martensitic steel B shows linear decrease up to 500 °C due to annealing processes – exceeding this temperature the hardness drops more rapidly due to further microstructural changes. Ferritic-pearlitic steel C reveals softening due to the formation of globular Fe_3C [PAPER II].

Figure 1.15. Hot hardness tester (HHT): a – scheme of apparatus, b – image [41].

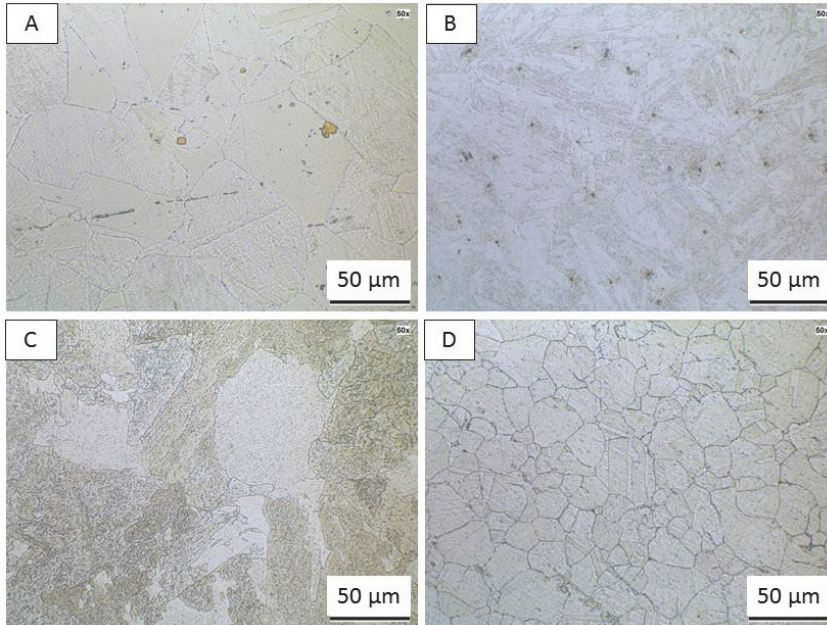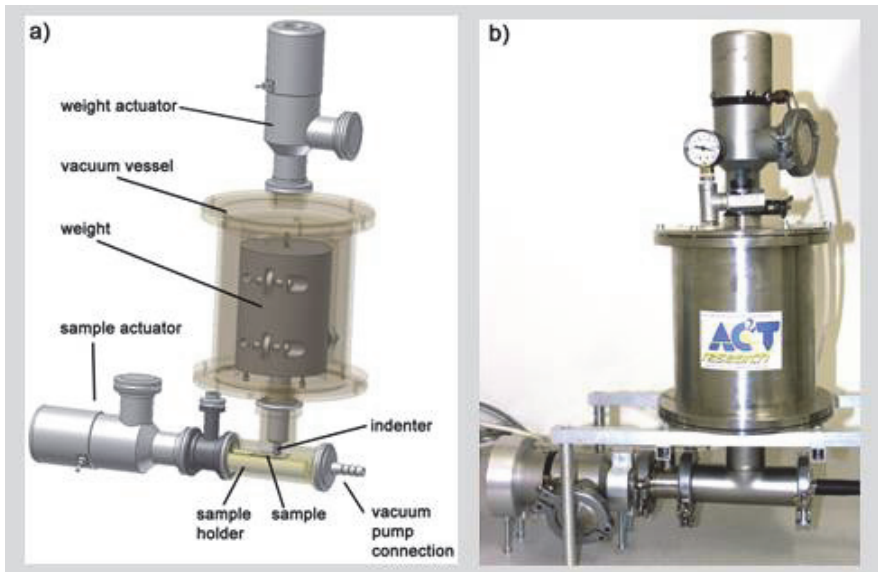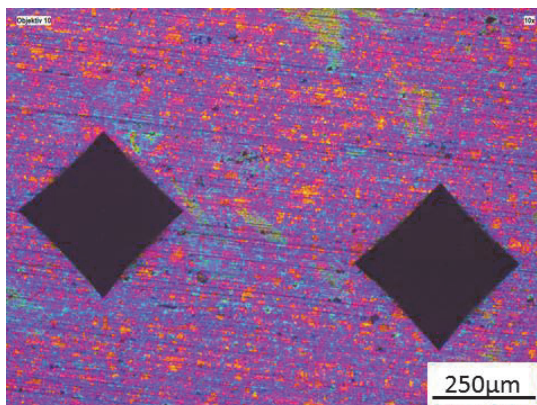*Figure 1.16. Image of HHT indents of steel (D) austenitic steel X8CRNINB16-13.*
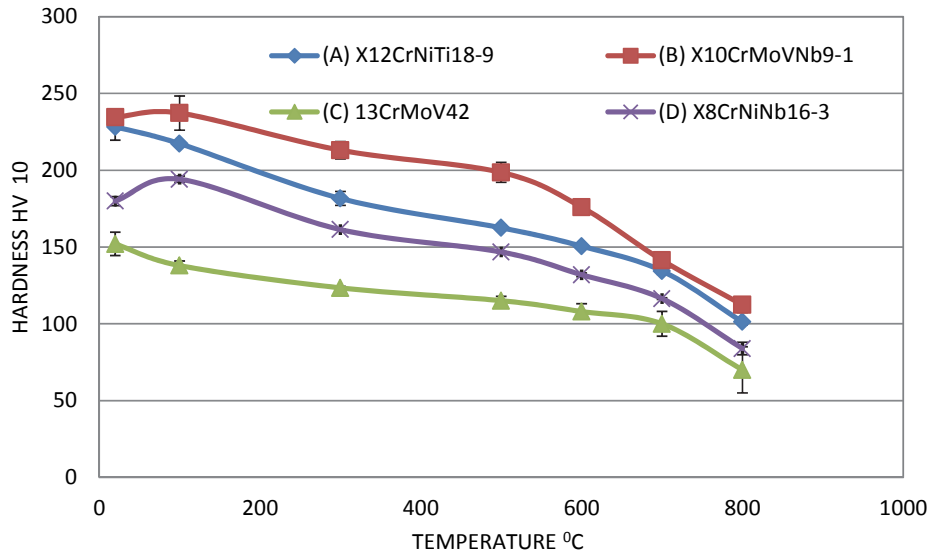
Figure 1.17. Hot hardness of steels investigated: (A) austenitic steel X12CrNiTi18-9, (B) martensitic steel X10CrMoVNb9-1, (C) pearlitic steel 13CrMoV42, (D) austenitic steel X8CrNiNb16-13 [PAPER II].

2 HIGH TEMPERATURE CORROSION TESTING

2.1 Corrosion tester and experiments

The high temperature corrosion tests of all steels investigated were carried out within the newly developed HTC tester. The test rig is mainly based on a furnace with a thermal protection, a gas feed and cleaning unit. A detailed scheme for the HTC tester is given in Figure 2.1. The test rig is based on a horizontal furnace equipped with a ceramic working tube. This furnace enables gaseous corrosion testing up to 1500 °C with randomly mixable gasses. The temperature and flow of corrosive gases are automatically controlled. The gasses are fed into the furnace through a thermal protection, where the samples are embedded in crucibles. At the other side of the heated tube, there is also a thermal protection including a gas cleaning unit, for high process reliability and workspace security. To ensure highest security for operators and the surrounding laboratories, the whole test rig is implemented in a protection chamber with an alarm system [PAPER I].

Within this study experiments were performed at 500 °C and 600 °C with an exposure time of 19 h. The corrosion tests have been performed on grinded specimens (25x15x6 mm), which have been cut from original boiler tubes. Prior to the tests all specimens were ultrasonically cleaned with ethanol, precisely measured by a calliper and weighed. After that, the samples were coated by manual brushing with a suspension of oil shale ash and ethanol for the optimal simulation of oil shale ash on-tube deposits for the corrosion tests. The tests were carried out in the temperature-controlled horizontal tube furnace of the HTC tester. For the experiments HCl was passed through the chamber at a velocity of 1,9 cm/s. The samples were positioned vertically and parallel to the flow direction. After the test procedure the samples were weighed, determining the mass gain for the calculation of the corrosion rates. For the experiments in oxidative environment, the samples were given into a furnace at 500 °C and 600 °C for 24h in synthetic air atmosphere (O_2~20 %, N_2~80 %). The oxidation tests have been done and the characterization was studied quantitatively by determining the samples mass increase [PAPER I].
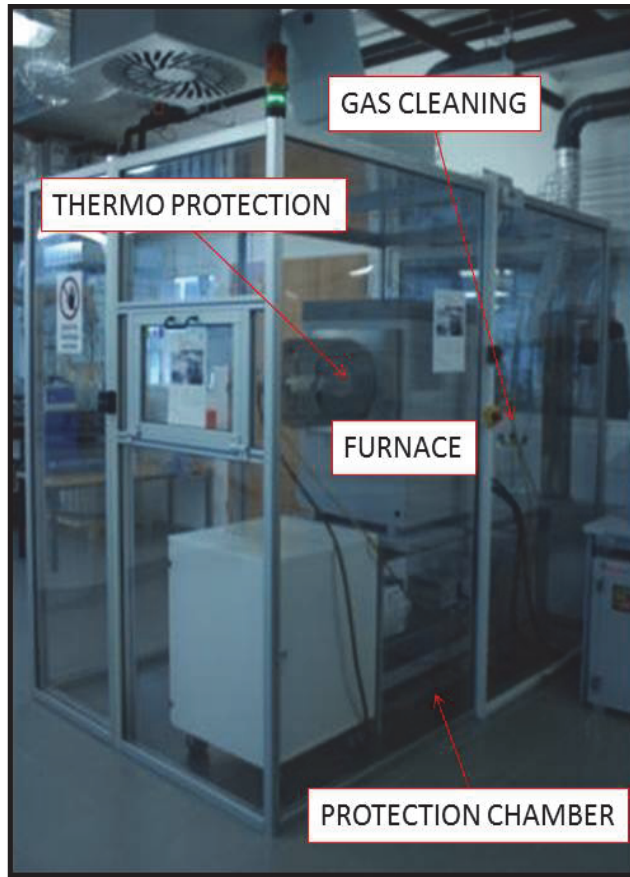
Figure 2.1. The HTC tester illustration.
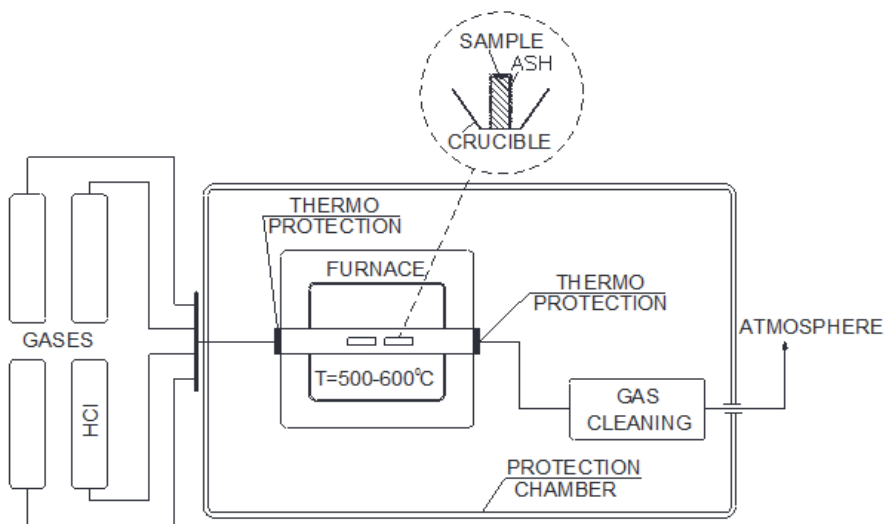
Figure 2.2. The HTC tester [PAPER I].
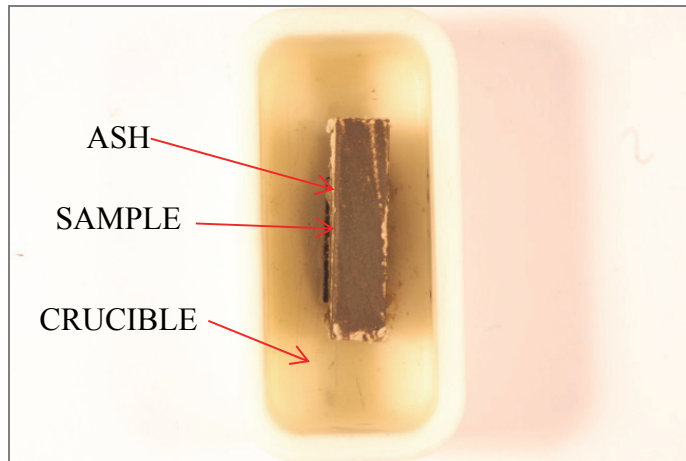
Figure 2.3. Sample after HTC test.

2.2 Properties of the Estonian oil shale ash

For the lab tests oil shale ash was processed by co-firing oil shale and biofuel in a Narva Power Plant with a CFB boiler, as seen in Figure 1.6. The fusion temperature of this ash strongly depends on the chemical and mineralogical composition of the ash. The main components of the Estonian oil shale ash which influence the ash fusibility are CaO, SiO_2 and Al_2O_3. Mineral matter in oil shale matter is a heterogeneous system containing minerals of carbonatic and sandy-clay nature. Due to the heterogeneity of different mineral matter in oil shale different fusion temperatures can occur [2]. In general, the fusion temperature for oil shale ashes and their components is higher than 1000 °C [39].

After the firing/processing an electrostatic precipitator (Figure 1.6 – pos. 11) was used to separate oil shale ash with a particle size from 45–60 μm. These oil shale ash particles were used for the corrosion tests in the HTC tester [42].

The chemical composition of the ash, analyzed by methods of analytical wet chemistry presented in Table 2.1:

Table 2.1. Chemical composition of the ash [PAPER I].

Components	%	Components	%
$CO2$	5.11 %	CaO_v	10.80 %
$C_{elem\ (CO2)}$	1.37 (5.04) %	CaO	29.40 %
$SO_{3\ common\ (Scom)}$	6.58 (2.63) %	MgO	5.63 %
$S_{sulphate}$	1.86 %	K_2O	4.10 %
$S_{sulphite}$	0 %	Na_2O	0.25 %
SiO_2	35.72 %	Cl	0.50 %
Fe_2O_3	5.33 %	Unburned parts	5.60 %
Al_2O_3	8.47 %		

2.3 Results and discussion

Mass change due to high temperature HCl corrosion in Estonian oil shale ash and oxidation

The mass gain depends on types of formed oxides (FeO, Fe_2O_3, Fe_3O_4, etc.) so the precise corrosion rate based on the determined mass gain is not possible without determination of above mentioned compounds and may be used for preliminary ranking of steel HTC resistance. For a more precise assessment of the steels HTC resistance, oxide layer was removed with an etchant and after the complete removal according to [42] the total mass loss was determined. Therefore a methodology using a 20 % aqueous Di-ammonium hydrogen citrate $[(NH_4)_2HC_6H_5O_7]$ solution was used to remove the oxide layer from all surfaces. Etching was conducted at 80 °C with several repetitions. Every etching cycle had a duration of 30 minutes. Figure 2.4 shows consistent decrease of the samples mass due to the oxide layer removing process. The mass gain of tested samples before etching the samples and the total mass loss due to HTC are presented in Figure 2.5.
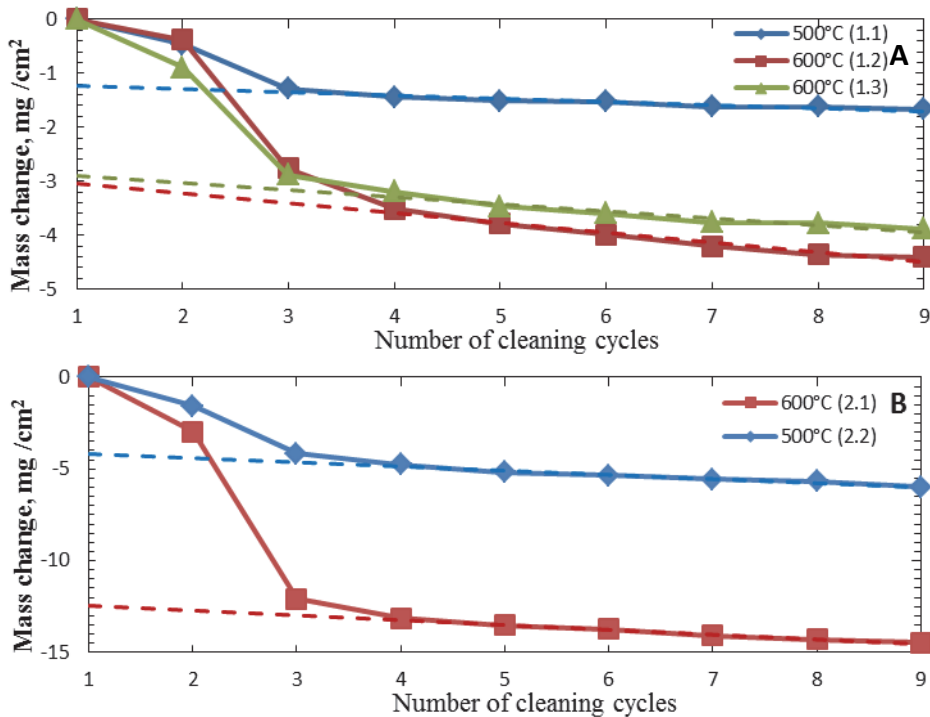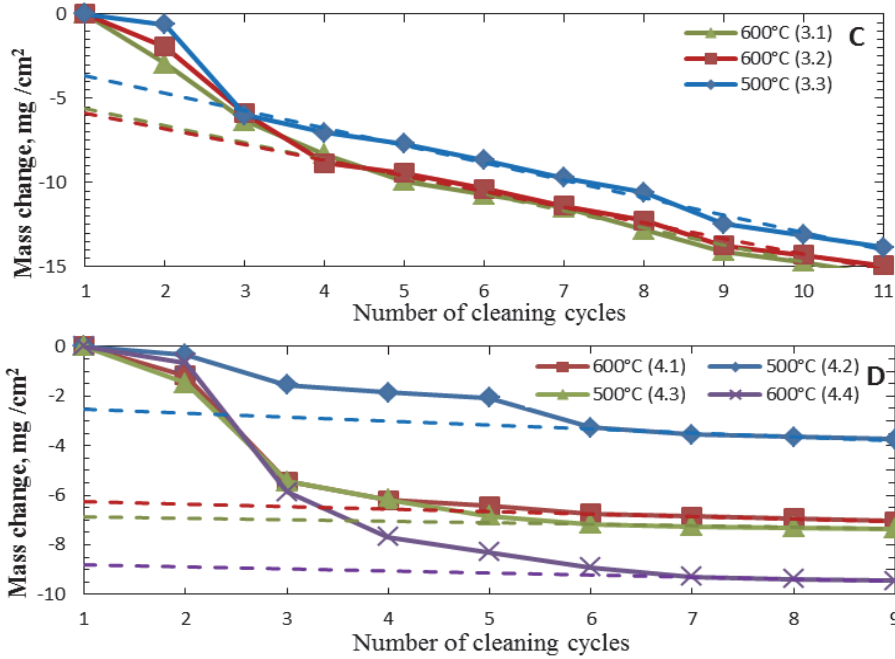
Figure 2.4. Relative mass changes of the steels investigated under HCl corrosion at 500 °C and 600 °C after corrosion layer removing, 1.1–1.3, 2.1–2.2, 3.1–3.3, 4.1–4.4 are number of the samples [PAPER I].
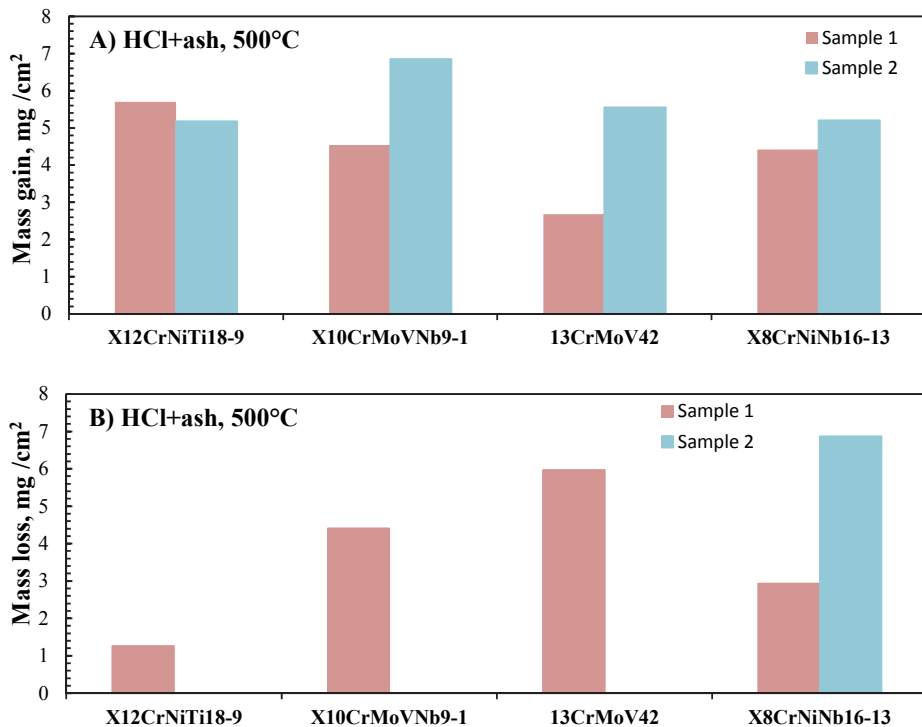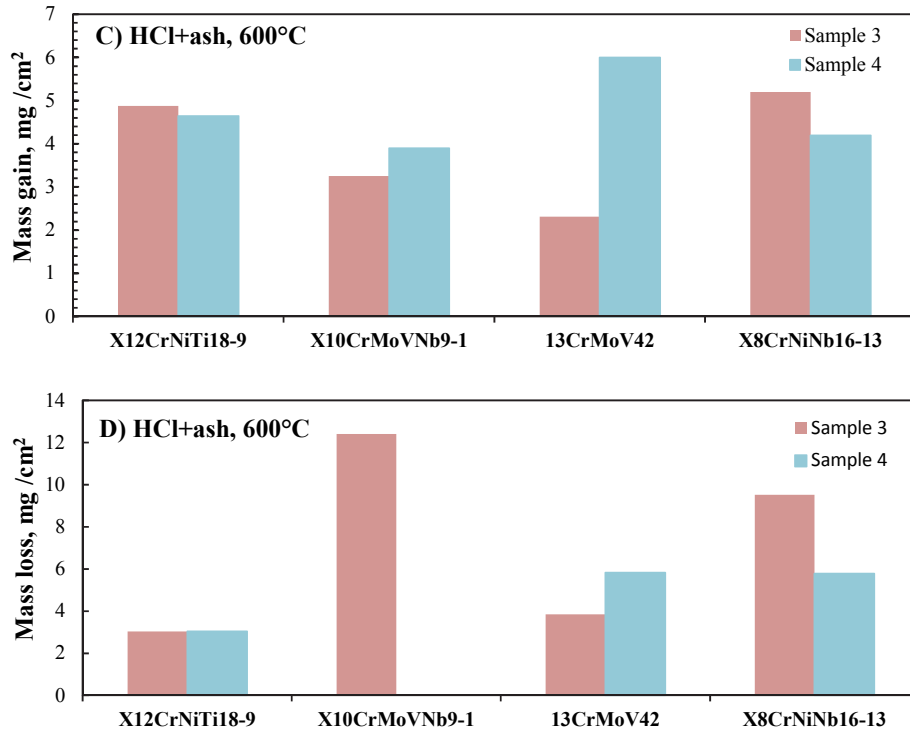
Figure 2.5. Mass loss and mass gain of the steels investigated under HCl corrosion at 500 °C and 600 °C after oxide layer removing [PAPER I].

One specimen of each steel was chosen for SEM-investigations – Therefore the sample was embedded and grinded/polished for optimal examination of the built-up corrosion products. Metal mass loss of specimen divided by specimen area allows obtaining the corrosion depth according to the following equations 2.1 and 2.2 [43]:

$$\Delta S = 1.28 \cdot \Delta m \text{ [mm] for carbon steels and medium-alloy pearlitic steels} \quad (2.1)$$
$$\Delta S = 1.25 \cdot \Delta m \text{ [mm] for high-alloy martensitic and austenitic steels} \quad (2.2)$$

Corrosion depths of all samples in HCl atmosphere and in Estonian oil shale ash are presented in Table 2.2 and Figure 2.6.

Table 2.2. Corrosion depth of the samples in HCl atmosphere and oil shale ash; Values given in [mm] [PAPER I].

Steel type	500 °C	600 °C	Steel type	500 °C	600 °C
A	0.00163 -	0.00378 0.00390	C	0.00492 -	0.00764 0.00782
B	0.00550 -	0.01550 -	D	0.00367 0.00782	0.00860 0.01100

33

Figure 2.6 a — Corrosion depth vs. Time for (A) X12CrNiTi18-9, (D) X8CrNiNb16-13

Legend:
- X12CrNiTi18-9, 500°C (TUT)
- X12CrNiTi18-9, 600°C (TUT)
- X12CrNiTi18-9, 500°C (fit)
- X12CrNiTi18-9, 600°C (fit)
- X12CrNiTi18-9, 500°C (AC2T)
- X12CrNiTi18-9, 600°C (AC2T)
- X8CrNiNb16-13, 500°C (AC2T)
- X8CrNiNb16-13, 600°C (AC2T)

2.6 a

Figure 2.6 b — Corrosion depth vs. Time for (B) X10CrMoVNb9-1

Legend:
- 620°C (TUT)
- 580°C (TUT)
- 540°C (TUT)
- 600°C (AC2T)
- 500°C (AC2T)
- 620°C (TUT, fit)
- 580°C (TUT, fit)
- 540°C (TUT, fit)

2.6 b

Figure 2.6. Results of the HTC Tests in presence of Estonian oil shale ash in AC^2T and in DTE TUT laboratories [34].

To compare the results of laboratorial methods determining the high temperature corrosion of steels, which were performed at the Department of Thermal Engineering, Tallinn University of Technology (DTE TUT) [31–34] results of both test series are given in Figure 2.6. As seen in this graphs, the results of DTE TUT laboratory tests are presented as kinetic diagrams of corrosion depth in coordinates ln ΔS - ln τ. In logarithmic coordinates the kinetic lines of high temperature corrosion are straight lines and usually expressed by following empirical correlation (2.2) [31–34].

Coefficients of graphs 2.6a and 2.6b are determined experimentally, at graph 2.6c is used coefficients specified in [43].

As it could be seen from Figure 2.6a the results of present experimental of steel A (12X18H10T) are in good agreement with the results of DTE TUT laboratory tests of this steel. Compared to steel A the corrosion depths of steels B, C and D are much higher [PAPER I].

In Figure 2.6b are presented steel grade B (X10CrMoVNb9-1) AC^2T experimental HTC results in comparison with the results of DTE TUT [44]. It is seen that corrosion depth at temperature 600 °C (AC^2T experiments) is a little higher than it was measured in DTE TUT at temperature 580 °C and 620 °C. Corrosion depth at temperature 500 °C (AC^2T experiments) is lower than DTE TUT at temperature 540 °C. So in case of steel grade X10CrMoVNb 9-1 it could be found good agreement with previous results as well.

In Figure 2.6c are presented steel grade C (13CrMoV42) AC^2T experimental HTC results in comparison with the PTM empirical correlation [43] based on

HTC tests of this steel under effect of oil shale ash provided in DTE TUT. It is seen that corrosion depth at temperature 500 °C is in good agreement with empirical correlation and at temperature 600 °C is significantly lower.

In conclusion of comparative analysis of HTC experimental results it should be emphasized that the results of HTC experiments, which have been carried out in laboratory AC^{2}T are in a good agreement with results obtained from the tests conducted in DTE TUT for three investigated steels. The HTC tests in AC^{2}T have been carried out in the media of gaseous HCl and oil shale ash, while the tests in DTE TUT have been performed in the media of natural gas combustion products and periodically renewable oil shale ash. Thus a good agreement of the results allows to consider used in AC^{2}T technique for HTC investigation as a valid one and the results to be reliable. Moreover the AC^{2}T technique has an advantage in comparison with DTE TUT technique because it does not require periodical interrupting of the experiment for oil shale ash renewal. HTC laboratory tests of investigated boiler steel grades in the presence of sulphur and potassium containing oil shale ash have shown that the best corrosion resistant is austenitic steel grade (A) X12CrNiTi18-9, then are going austenitic steel (D) X8CrNiNb16-13, pearlitic steel grade (C) 13CrMoV42 and martensitic (B) X10CrMoVNb9-1. That sequence represents the corrosion ranking of the tested steel grades for their application as high-temperature heating surfaces in boilers firing oil shale which contain chlorine, sulphur and potassium in outer deposits.

Obtained ranking and HTC tests results could be used for selection of steel for boiler components designed for operation in similar conditions.

In order to make more precise life time assessment of component operated in HTC conditions in the presence of oil shale ash deposits the long term field tests are required.

In high temperature oxidative environment all steels show mass increase due to the formation of oxide surface layer. The mass changes of all steels investigated are given in Figure 2.7.
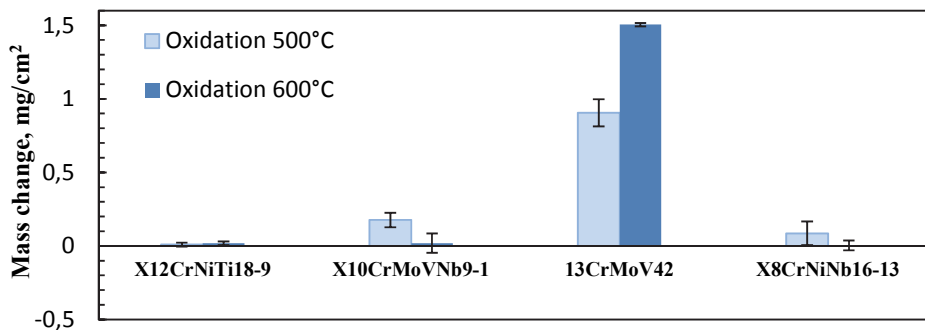

Figure 2.7. Mass changes of the steels investigated in oxidative environment at 500 °C and 600 °C for 24h [PAPER I].

As seen in the figure, steel C show the highest mass increase due to the lowest amount of alloying elements like chromium and nickel, which can decrease

oxidation due to the formation of dense layers [PAPER I]. The ranking of steel grades resistance in high temperature oxidative environment (air) in the laboratory conditions was as follows: the best resistant is austenitic steel grade (A) X12CrNiTi18-9, then are going austenitic steel (D) X8CrNiNb16-13, martensitic (B) X10CrMoVNb9-1 and pearlitic steel grade (C) 13CrMoV42.

2.4 Qualitative analysis of the formed corrosion layer using scanning electron microscopy

In the following chapter the effects of high temperature corrosion of the investigated steels are shown and discussed. Qualitative analyses were performed to understand high temperature corrosion of the presented steels using a scanning electron microscope (SEM) "Zeiss FESEM Gemini Supra VP" and energy dispersive X-Ray spectroscopy (EDX) [PAPER I].

Prior to the removal of the built-up scales the surface of the corroded samples were analyzed by SEM/EDX. Metallographic cross sections of the corroded samples were prepared to analyze formed layers and the corrosive behavior of different phases from all steels investigated. In Figure 2.9 and Figure 2.10 analysis of a surface of the samples after exposure are observed after the tests at 500 °C and 600 °C. In Figure 2.8 and in Figures 2.11 – 2.18 cross-sectional analysis of the steels investigated are given. The oxide layer formed after 500 °C and 600 °C corrosion test for 24h is different for austenitic, pearlitic and martensitic steels [PAPER I].

As mentioned above, the corrosion layer thickness strongly depends on chemical composition of steels. Steels (A) austenitic X12CrNiTi18-9 alloy and (D) austenitic X8CrNiNb16-13alloy consist of 18.48 % / 18.64 % of chromium (Cr) and 10.39 % / 11.19 % of nickel (Ni) [PAPER I].

Steel A Figure 2.11, 2.15 shows a well visible sublayer at the boundary between the base metal and the oxide layer which is damaged by pores and cracks formed according to above described corrosion process. Chlorides which penetrate through the base material at 500 °C cause a porous sublayer at the boundary. The thickness of this porous sublayer may be estimated as 5 μm, at the temperature of 600 °C increases up to 7 – 9 μm – locally the sublayer disappeared completely [PAPER I].

Steel B, a martensitic steel X10CrMoVNb9-1 alloy consist 8.86 % of chromium and 1.08 % of molybdenum. As seen in Figure 2.12, 2.16 the boundary between the base metal and the oxide layer is a well visible sublayer damaged by pores and cracks. The uneven surface of the base metal indicates to a different corrosion rate along the surface of the sample. At 500 °C the thickness of the porous sublayer can be estimated to ~10 μm, at 600 °C increases up to 20-25 μm [PAPER I].

Steel C, Figure 2.13, 2.17 the pearlitic steel 13CrMoV42 did not built-up any protective oxide layer at both temperatures (500 °C and 600 °C) because of low contents of heat-resisting alloying elements such as chromium (1.44 %). Porous sublayer between the base metal and the oxide layer cannot be detected, but the corrosion develops quite uniformly along the sample surface [PAPER I].

The influence of volatile chlorides, especially chromium chlorides, on the corrosion mechanism in this case is at a minimum wage due to the low chromium content in the bulk. The corrosion rate of this low alloyed steel grade in HCl environment is comparable to the corrosion of higher alloyed austenitic steels and lower than those for martensite, due to the same low resistance against gaseous HCl at elevated temperatures due to the lack of protective layers which can resist the chlorine attack [PAPER I].

Steel D Figure 2.14, 2.18: At 500 °C the thickness of the porous sublayer can be estimated as 5 – 7 µm, at 600 °C increases up to 10 – 15 µm. In this sublayer many pores are visible throughout the whole samples. Those significant difference in the HTC rate between two austenitic steel grades (having about the same content of Chromium and Nickel but with different elements used for stabilization of the structure) can be pointed out to the formation of less resistant layers at steels D and the higher amount of nickel, which more easily forms chlorides than chromium and the resulting formation of porous sublayers [PAPER I].
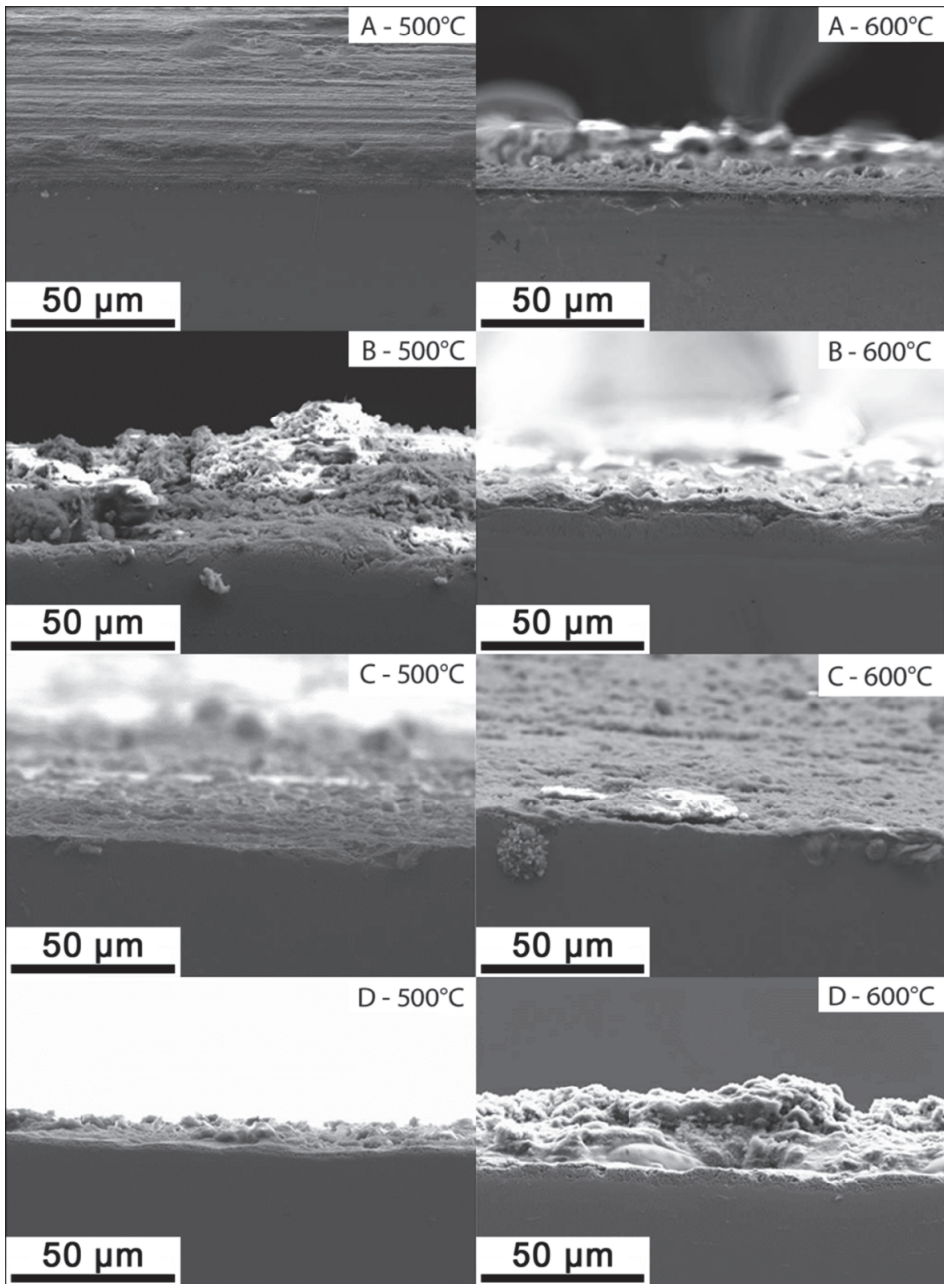
Figure 2.8. Scanning electron microscopy (SEM) surface cross-sectional analysis of the oxide layer formed after corrosion tests at 500 °C (1) and 600 °C (2) for 24h on steels: (A) austenitic steel X12CrNiTi18-9, (B) martensitic steel X10CrMoVNb9-1, (C) pearlitic steel 13CrMoV42, (D) austenitic steel X8CrNiNb16-13.
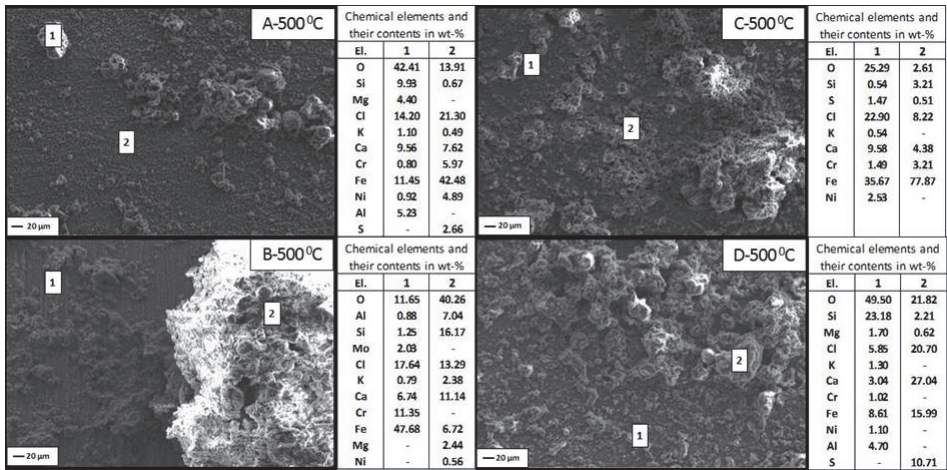
Figure 2.9. Scanning electron microscopy (SEM) surface analysis of the sample after corrosion tests at 500 °C for 24h on steels: (A) austenitic steel X12CrNiTi18-9, (B) martensitic steel X10CrMoVNb9-1, (C) pearlitic steel 13CrMoV42, (D) austenitic steel X8CrNiNb16-13[PAPER I].

A-500°C — Chemical elements and their contents in wt-%

El.	1	2
O	42.41	13.91
Si	9.93	0.67
Mg	4.40	-
Cl	14.20	21.30
K	1.10	0.49
Ca	9.56	7.62
Cr	0.80	5.97
Fe	11.45	42.48
Ni	0.92	4.89
Al	5.23	-
S	-	2.66

C-500°C — Chemical elements and their contents in wt-%

El.	1	2
O	25.29	2.61
Si	0.54	3.21
S	1.47	0.51
Cl	22.90	8.22
K	0.54	-
Ca	9.58	4.38
Cr	1.49	3.21
Fe	35.67	77.87
Ni	2.53	-

B-500°C — Chemical elements and their contents in wt-%

El.	1	2
O	11.65	40.26
Al	0.88	7.04
Si	1.25	16.17
Mo	2.03	-
Cl	17.64	13.29
K	0.79	2.38
Ca	6.74	11.14
Cr	11.35	-
Fe	47.68	6.72
Mg	-	2.44
Ni	-	0.56

D-500°C — Chemical elements and their contents in wt-%

El.	1	2
O	49.50	21.82
Si	23.18	2.21
Mg	1.70	0.62
Cl	5.85	20.70
K	1.30	-
Ca	3.04	27.04
Cr	1.02	-
Fe	8.61	15.99
Ni	1.10	-
Al	4.70	-
S	-	10.71

Figure 2.10. Scanning electron microscopy (SEM) surface analysis of the sample after corrosion tests at 600 °C for 24h on steels: (A) austenitic steel X12CrNiTi18-9, (B) martensitic steel X10CrMoVNb9-1, (C) pearlitic steel 13CrMoV42, (D) austenitic steel X8CrNiNb16-13[PAPER I].

A-600°C — Chemical elements and their contents in wt-%

El.	1	2
O	43.98	19.38
Si	15.92	3.91
Mg	2.18	0.89
Cl	10.30	20.57
K	1.19	1.21
Ca	13.21	33.15
Cr	3.22	6.69
Fe	2.56	2.54
Mn	0.56	0.66
Al	6.89	1.27
P	-	9.73

C-600°C — Chemical elements and their contents in wt-%

El.	1	2
O	22.57	42.19
Cl	5.50	9.95
Ca	1.95	16.96
Fe	68.92	9.46
Mg	1.06	-
Al	-	5.71
Mg	-	1.70
K	-	1.18
Si	-	12.86

B-500°C — Chemical elements and their contents in wt-%

El.	1	2
O	11.65	40.26
Al	0.88	7.04
Si	1.25	16.17
Mo	2.03	-
Cl	17.64	13.29
K	0.79	2.38
Ca	6.74	11.14
Cr	11.35	-
Fe	47.68	6.72
Mg	-	2.44
Ni	-	0.56

D-600°C — Chemical elements and their contents in wt-%

El.	1	2
O	32.95	13.97
Si	8.39	-
Mg	11.20	-
Cl	7.83	8.25
K	0.18	0.27
Ca	13.72	2.23
Cr	1.63	10.39
Fe	15.43	53.19
Al	2.59	-
S	5.59	2.25
Ni	-	9.45

Figure 2.11. Scanning electron microscopy (SEM) cross-sectional analysis of the corrosion layer after the high temperature corrosion tests at 500 °C: (A) austenitic steel X12CrNiTi18-9 [PAPER I].

Figure 2.12. Scanning electron microscopy (SEM) cross-sectional analysis of the corrosion layer after the high temperature corrosion tests at 500 °C: (B) martensitic steel X10CrMoVNb9-1[PAPER I].

Figure 2.13. Scanning electron microscopy (SEM) cross-sectional analysis of the corrosion layer after the high temperature corrosion tests at 500 °C: (C) pearlitic steel 13CrMoV42 [PAPER I].

Figure 2.14. Scanning electron microscopy (SEM) cross-sectional analysis of the corrosion layer after the high temperature corrosion tests at 500 °C: (D) austenitic steel X8CrNiNb16-13[PAPER I].

Figure 2.15. Scanning electron microscopy (SEM) cross-sectional analysis of the corrosion layer after the high temperature corrosion tests at 600 °C: (A) austenitic steel X12CrNiTi18-9 [PAPER I].
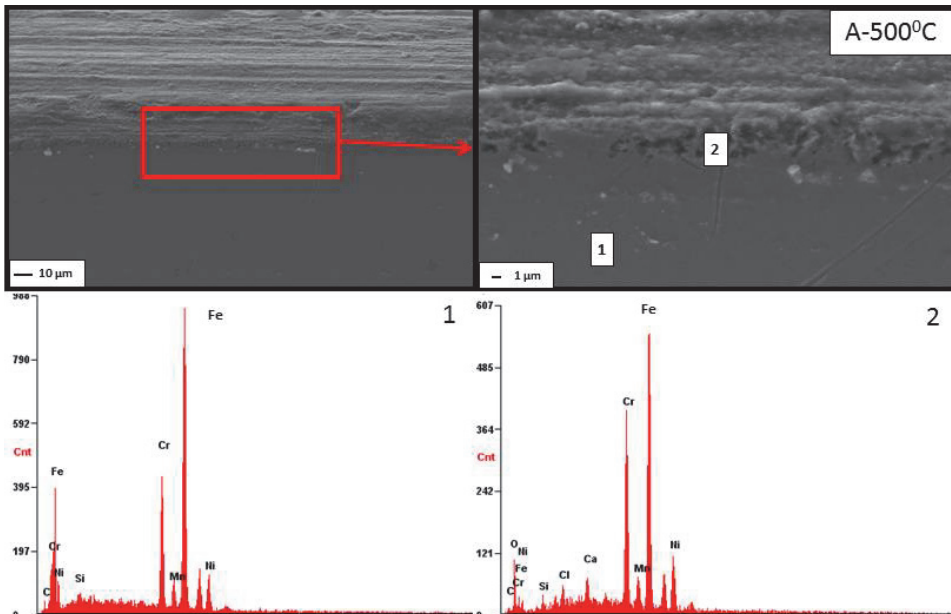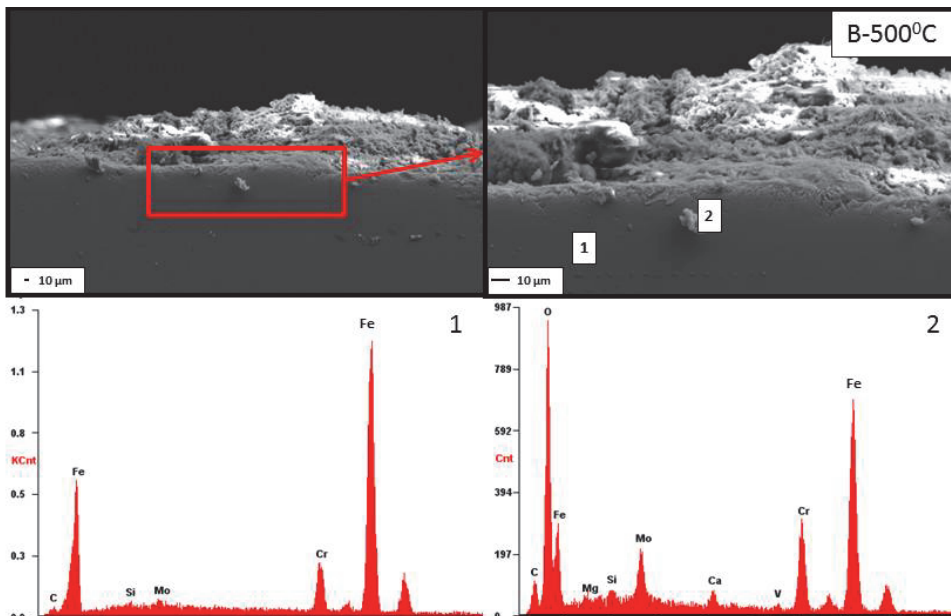

Figure 2.16. Scanning electron microscopy (SEM) cross-sectional analysis of the corrosion layer after the high temperature corrosion tests at 600 °C: (B) martensitic steel X10CrMoVNb9-1 [PAPER I].

Figure 2.17. Scanning electron microscopy (SEM) cross-sectional analysis of the corrosion layer after the high temperature corrosion tests at 600 °C: (C) pearlitic steel 13CrMoV42 [PAPER I].
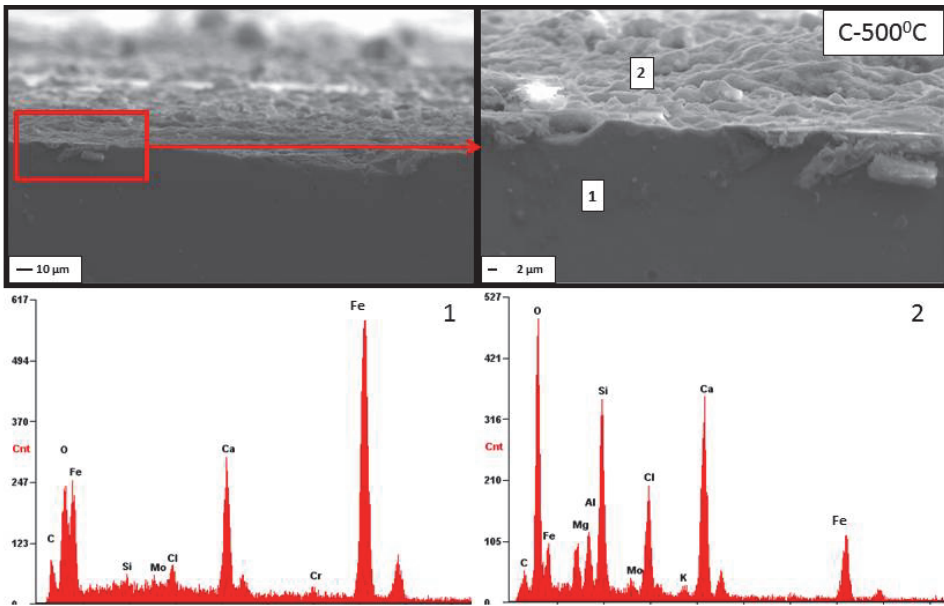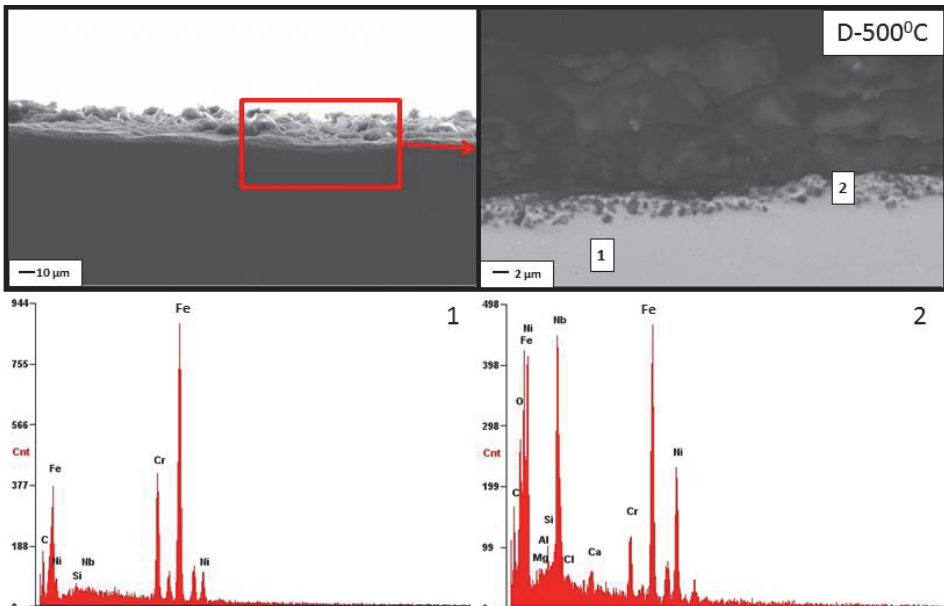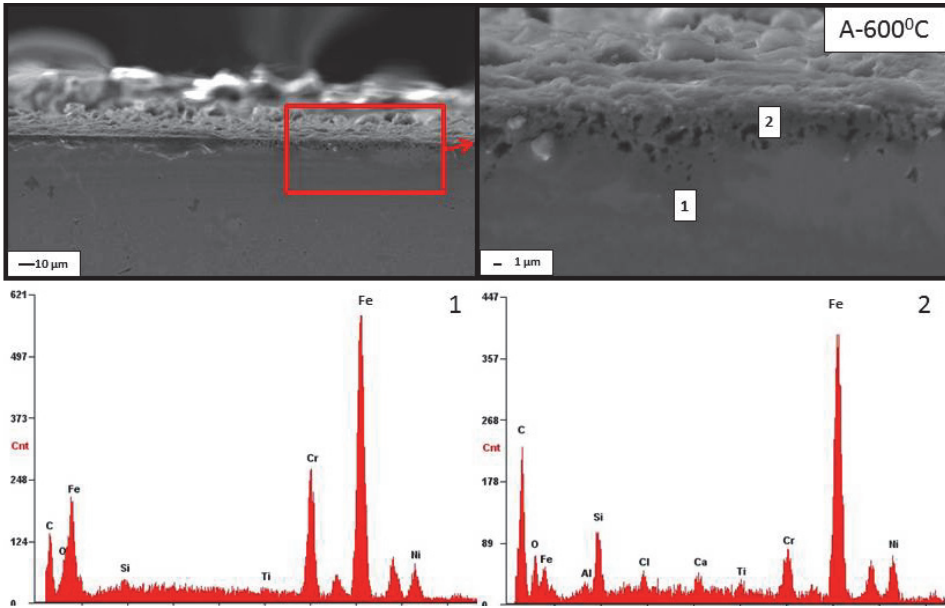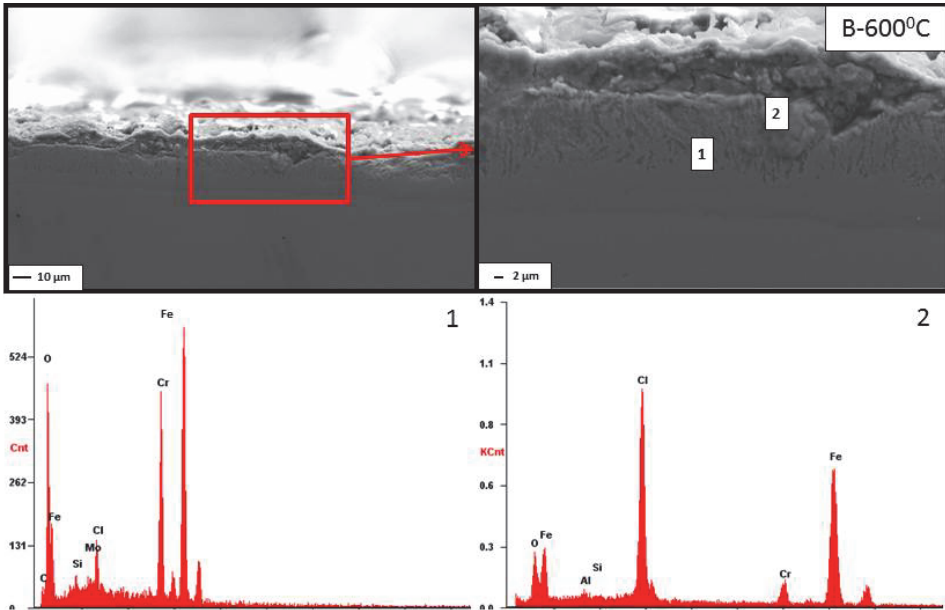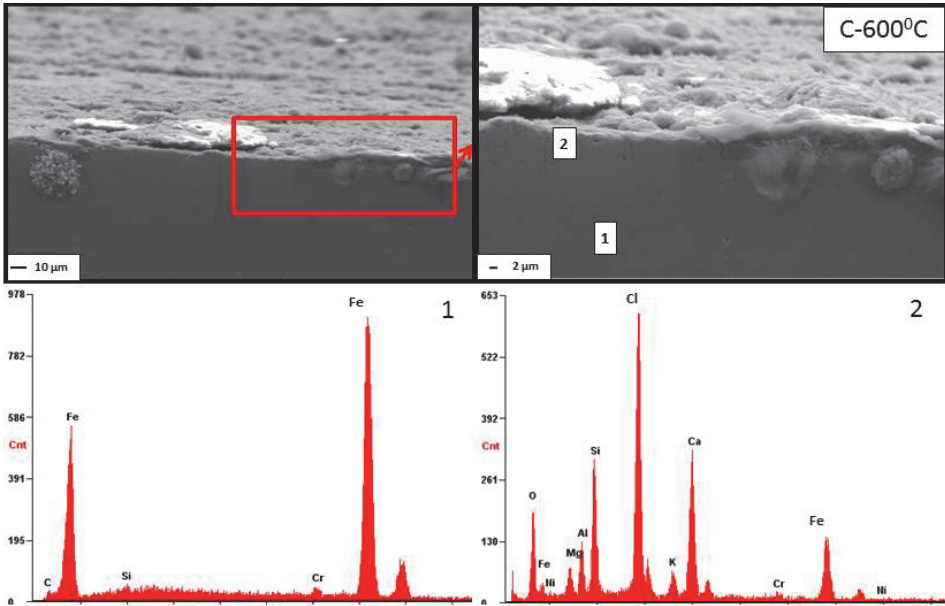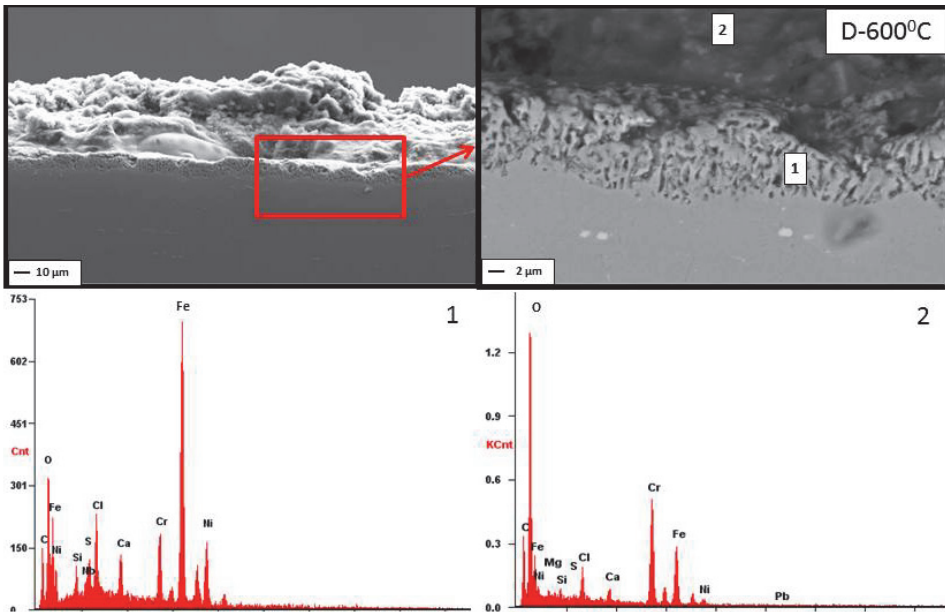

Figure 2.18. Scanning electron microscopy (SEM) cross-sectional analysis of the corrosion layer after the high temperature corrosion tests at 600 °C: (D) austenitic steel X8CrNiNb16-13[PAPER I].

Influence of the ash deposits on the corrosion of boiler steels

The protective properties of deposits, arising on a superheater surface, strongly depends on the properties of the surface, the content of alloying elements in a formed oxide layer, its porosity, the presence of crack and the character of cohesion of a layer with the base metal. In general alloying elements migrate from the base metal into the oxide layer, and their content in a layer is correlated with its content in the base metal and face temperature, remaining constant along the thickness of oxide layer [34, 44]. However, if external deposits on tubes contain chlorine compounds the corrosion processes and the resulting phenomena essentially are changed. The compounds of chlorine force a chemical reaction with both, chrome and iron. A counter migration takes place; chlorine migrates from the surface into the oxide layer and further to the base metal of the tube. Alloying elements migrate in an opposite direction [30].

The main components in an oxide layer, which decreases the velocity of the corrosion process in steels, is chromium oxide Cr_2O_3 and the mixed phases like $NiCr_2O_4$ and $FeCr_2O_4$ which at the presence of chlorine will form compound $CrCl_3$ volatilize from the tube surface [46]. Compounds like $FeCl_3$, CrO_2Cl_2, CrO_3, $NiCl_2$ etc. similarly volatilize. Thereby the oxide layer becomes porous, with low anti-corrosive protective properties, and KCl can easily diffuse through the pores to more cold layers of tube. Further, the present chlorides react with the gaseous combustion atmosphere and the oil shale, which both are sulphur containing. The elevated temperatures during the combustion process can turn the built-up chlorides into sulphates [31].

In the present experiments hot corrosion involves corrosion reactions between molten salts, oxidation, sulphatation and gaseous corrosion. In environment like air, the normal oxide scale which forms at the surface of an alloy acts as an effective barrier to further oxidation [15].

In practice, the oxide scale often becomes porous and cracked, allowing much faster transport along these channels. When molten salts are present, the salt wets the surfaces of the oxides and enables the corrosive anions to penetrate deep into and through the pores and cracks by capillary action [15].

In presented corrosion experiment no oxygen (O_2) was added into the gas flow, pure hydrogen chlorine (HCl) was reacted with steels covered with oil shale ash. The reaction with gas (HCl) and ash, containing sulphides leads to salts formation. Under high temperature melting salts localized molten salts corrosion is the main damaging mechanism, which can be present in all phases occurring in a material [45].

On the basis of conducted experiments have been found:

- HTC tests of investigated boiler steel grades in the presence of sulphur and potassium containing oil shale ash in HCl environment have shown that the best corrosion resistant is austenitic steel grade (A) X12CrNiTi18-9, then are going austenitic steel (D) X8CrNiNb16-13, pearlitic steel grade (C) 13CrMoV42 and martensitic (B) X10CrMoVNb9-1. That sequence represents the corrosion ranking of the tested steel grades for their

application as high-temperature heating surfaces in boilers firing oil shale which contain chlorine, sulphur and potassium in outer deposits.

- The ranking of steel grades resistance in high temperature oxidative environment (air) was as follows: the best resistant is austenitic steel grade (A) X12CrNiTi18-9, then are going austenitic steel (D) X8CrNiNb16-13, martensitic (B) X10CrMoVNb9-1 and pearlitic steel grade (C) 13CrMoV42.

Performance maps

In order to make reasonable selection of relevant steel grade in definite laboratory conditions the corrosion-oxidation performance maps (Figure 2.19, 2.20) have been proposed.

TEST CONDITIONS
500°C

CORROSION MASS LOSS [mg/cm²]	LOW 1.26	MEDIUM 4.41	HIGH 5.97	MEDIUM 6.87 2.93
OXIDATION MASS GAIN [mg/cm²]	LOW 0.0002	LOW 0.0018	HIGH 0.0091	LOW 0.0009
GRADE	A	B	C	D
TESTED	12X18H10T	X10CrMoVNb9-1	12X1MФ	TP347HFG
EQUIVALENT	X12CrNiTi18-9	P91	13CrMoV42	X8CrNiNb16-13

Figure 2.19. Performance map of studied steels at 500°C.

TEST CONDITIONS
600°C

CORROSION MASS LOSS [mg/cm²]	LOW 3.04 3.03	HIGH 12.42	MEDIUM 3.84 5.83	MEDIUM 9.52 5.78
OXIDATION MASS GAIN [mg/cm²]	LOW 0.0002	LOW 0.0002	HIGH 0.0015	LOW 0.0003
GRADE	A	B	C	D
TESTED	12X18H10T	X10CrMoVNb9-1	12X1MФ	TP347HFG
EQUIVALENT	X12CrNiTi18-9	P91	13CrMoV42	X8CrNiNb16-13

Figure 2.20. Performance map of studied steels at 600°C.

3   HIGH TEMPERATURE ABRASIVE WEAR

TESTING

3.1   Study of high temperature erosion

Erosion testing method

Solid particle erosion tests have been performed in a centrifugal four-channel accelerator (HTE) in which up to 20 specimens can be treated simultaneously under identical testing conditions (Figure 3.1). Prior to the tests all specimens were ultrasonically cleaned with ethanol, precisely measured by a calliper and weighed. The abrasive particles used in this work were rounded silica particles. Investigation of steady state erosion rate was made as a function of the impact angle at the abrasive particles velocity of 80 m/s [19]. Erosion at such a high speed was selected to reduce possible role of oxidation during erosion-oxidation process. Erosion tests were conducted at impact angles of 30° and 90°, respectively. The duration of each erosive test was approximately 1 hour. In each test, specimens of the size of 20x15x4.5mm were treated simultaneously. Parameters of the tests are given in Table 3.1 [46]. After the test procedure the samples were weighed, determining the mass loss.

Table 3.1. Testing parameters used in erosion testing [46].

Parameter	Value
Impact velocity	80 m/s
Impact angles	30°, 90°
Erodent	Silica sand
Total weight of erodent	6 kg
Test temperatures	500 and 600 °C
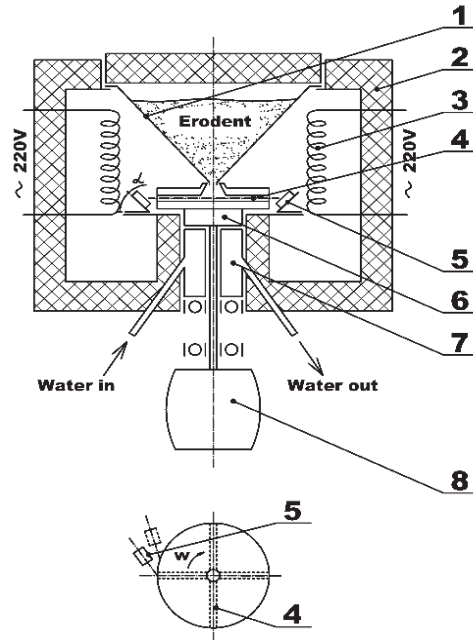
Figure 3.1. Scheme of erosion test apparatus: (1) abrasive bunker; (2) insulation; (3) heating elements; (4) rotor with channels; (5) specimen; (6) system to avoid vibration; (7) shaft cooling system; (8) el. motor [19].

Results of high temperature erosion of steels

The volumetric wear rate (K_{vol}) was determined as wear rate (K) of the target sample divided by steel density (Figure 3.2, 3.3).

$$K_{vol} = K/\rho \qquad [\text{mm}^3/\text{kg}] \qquad (3.1)$$

where wear rate (K) is calculated as following:

$$K = \Delta m/(G \cdot v) \qquad [\text{mg/kg}], \qquad (3.2)$$

where Δm – specimen weight loss [mg];
　　　 G – the quantity of sand [kg];
　　　 v – is share of sand per one specimen for elevated temperature tester ($v = 0.0187$).

An accuracy of 0.1mg was obtained for the target mass loss measurements.

The investigated steels show a change of the wear in the temperature range from 500 °C to 600 °C. Considering steels B, C and D volumetric wear rate for both tests increases with increasing temperature. Opposite behaviour can be detected for austenitic steel A which exhibits better wear performance at higher testing temperature of 600 °C in test with impact angle of abrasive 30° [46]. That may be explained by particle sticking (Figure 3.4 and 3.5).

Analyzing steels wear rate accordingly to impact angle of abrasive particle influence, it should be mentioned that wear rate is lower with impact angle of 90° for steels investigated [46].
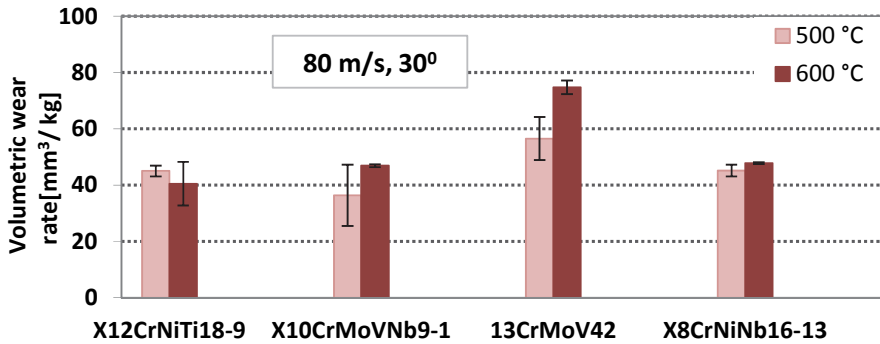
Figure 3.2. Volumetric wear rate of steels at elevated temperatures under the impact angles of 30° [45].
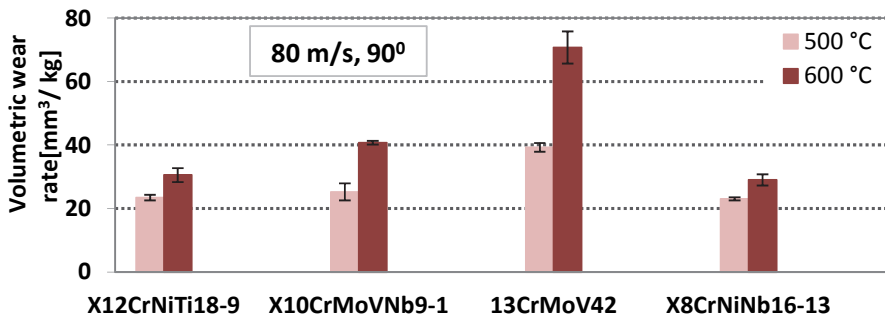
Figure 3.3. Volumetric wear rate of steels at elevated temperatures under the impact angles of 90° [46].

For better understanding of steels behaviour in erosive conditions the SEM analysis of samples after test was performed. A typical SEM images of steels are given at Figure 3.4 and 3.5. It can be clearly seen that abrasive SiO_2 particles embed into wear surface [46]. The worn surfaces of steel tested under 30° and 90° impact angles at elevated temperatures indicates a highly plastically deformed surface. The highest volumetric wear rate among the tested materials shows steel (C) 13CrMoV42 that may be explained by low hot hardness.
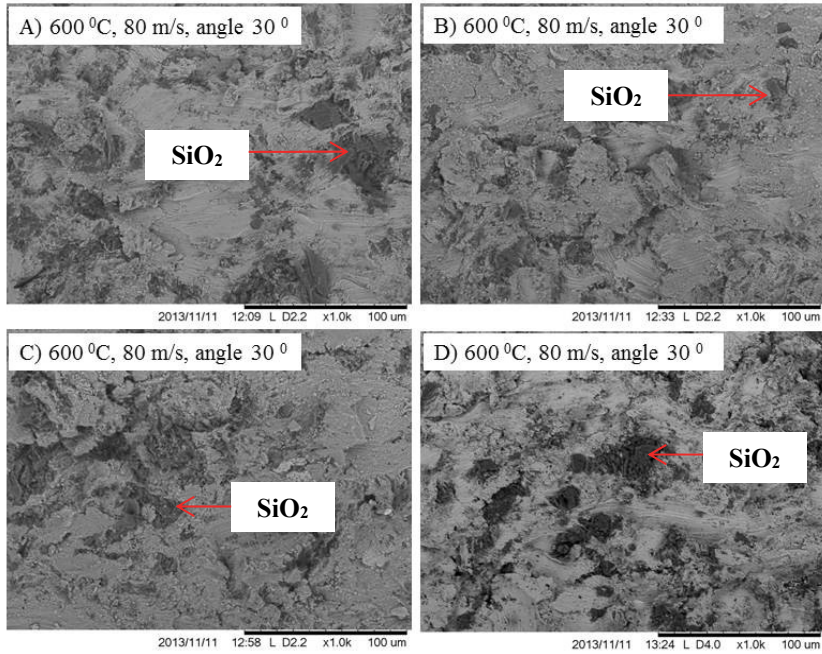
Figure 3.4. Worn surfaces of eroded steels at temperature 600 °C of impact angle 30°:(A) X12CrNiTi18-9, (B) X10CrMoVNb9-1, (C) 13CrMoV42, (D) X8CrNiNb16-13[46].
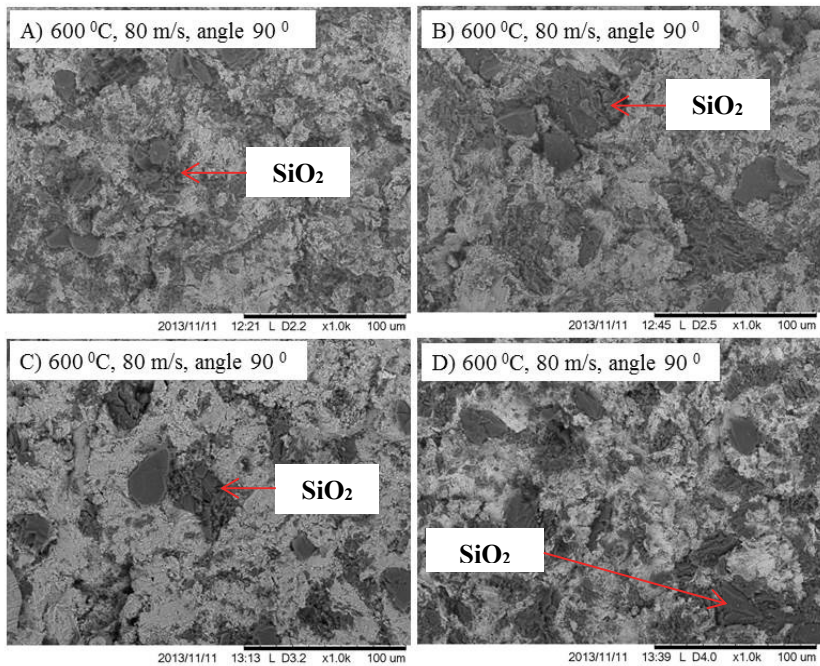
Figure 3.5. Worn surfaces of eroded steels at temperature 600 °C of impact angle 30°: (A) X12CrNiTi18-9, (B) X10CrMoVNb9-1, (C) 13CrMoV42, (D) X8CrNiNb16-13[46].

3.2 Study of high temperature abrasion wear

Cyclic-impact abrasion tester and experiments

For the high temperature cyclic impact abrasion (HT – CIA) testing apparatus (Figure 3.7a) of the Austrian Centre of Competence for Tribology (AC²T) was used to determine the behaviour of steels at elevated temperatures. Test principle is based on potential energy (0.8 J) which is cyclically turned into kinetic energy by free fall. Samples are fixed at 45° and are periodically hit by the plunger with 1.8 – 2.0 Hz frequency with a constant flow of abrasive (3 g/s, silica sand with particle size of 0.4 – 0.9 mm, Fig. 3.7c) between plunger and sample (Figure 3.7b) [24]. Tests were done at 500 °C and 600 °C. Prior to the tests all specimens were ultrasonically cleaned with ethanol, precisely measured by a calliper and weighed. After the test specimens were ultrasonically cleaned again and weighed. Wear was determined by mass loss and wear volume was calculated via steels density. The plunger material used for these tests was a Co-rich high-speed steel. Test duration was set constant to 1 h. The testing parameters are summarized in Table 3.6. The characterization of wear behaviour was done by determining the weight loss (accuracy 0.1 mg). Qualitative analysis were performed [PAPER II] by standard optical microscopy (Figure 3.9, 3.10) and by confocal microscopy Leica DCM 3D (Figure 3.12).

Table 3.6. Testing parameters of high-temperature cyclic impact abrasion [PAPER II].

Parameter	Value
Impact energy	0.8 J
Impact angle	45°
Frequency	1.8 – 2 Hz
Number of testing cycles	6900 – 7200
Abrasive, size, shape and hardness	Silica sand; 0.4 – 0.9 mm; angular; 1000 – 1200 HV
Abrasive flow	3 g/s
Test temperature	500 and 600 °C
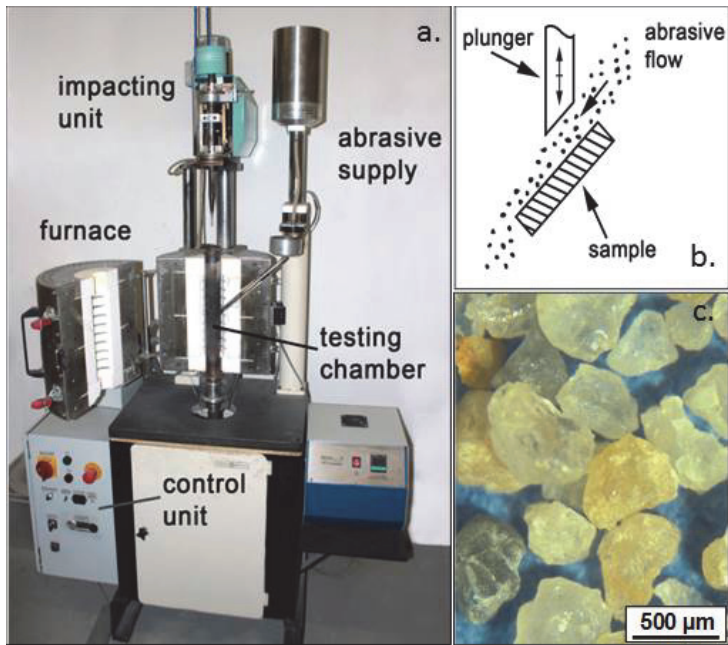
Figure 3.7. High-temperature cyclic impact abrasion (HT – CIA) test: a) view of the tester; b) testing principle; c) micrograph of abrasive particles [24].

Results of high-temperature impact-abrasion of steels

Qualitative analysis was performed by standard optical microscopy (Figure 3.9, 3.10) and by confocal microscopy Leica DCM 3D (Figure 3.12). The results of the HT – CIAT tests are displayed in Figure 3.8. The investigated steels show a significant change of the wear in the temperature range from 500 °C to 600 °C. Considering steels A, B and D that exhibit higher hot hardness values than steel C, volumetric wear increases with increasing temperature. It can be assumed that the volumetric wear increases due to softening effects of the microstructure. Opposite behaviour can be detected for the ferritic – pearlitic steel C which exhibits better wear performance at higher testing temperature of 600 °C. In order to deeper understand this effect SEM analyses of the wear scars in the different regions were performed for all steels. A typical SEM analysis of the worn surface of steel B is present in Figure 3.11a. It can be clearly seen that abrasive SiO_2 particles stuck in the wear surface in impact zone of the sample. EDS line scan analysis was done additionally to detect incorporate abrasive particles in the surface and near-surface region (Figure 3.11b). Low hot hardness of steel C allows a strong interaction of abrasive SiO_2 particles with the ductile surface zone within the impact region, resulting in a pronounced formation of a mechanically mixed layer which enables the protection of the material and reduction of the wear rate [PAPER II].
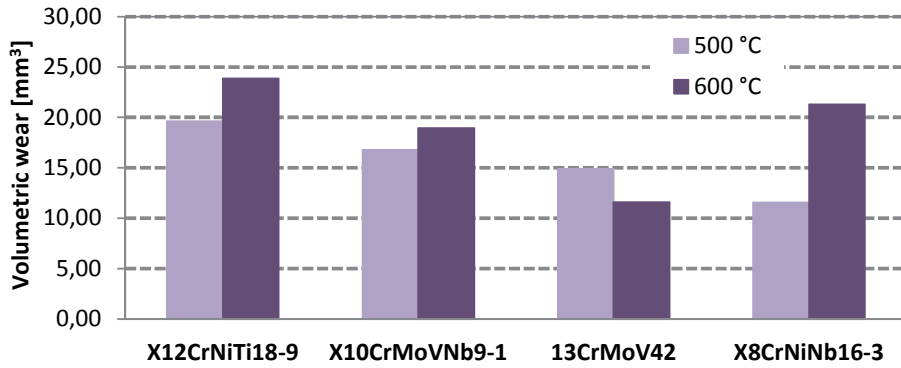
Figure 3.8. Volumetric wear of steels at elevated temperature under HT – CIA [PAPER II].
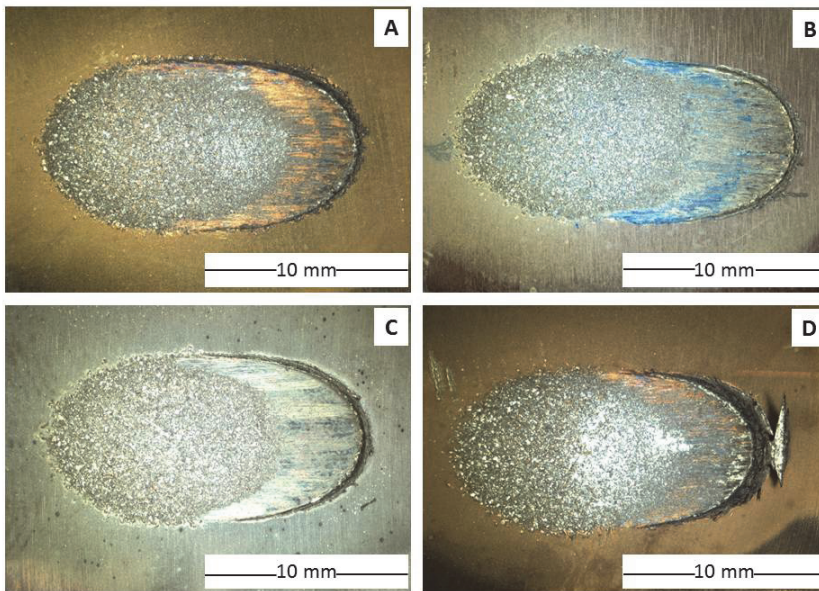
Figure 3.9. Macro images of typical wear scar of steel tested at 500 °C temperature: (A) X12CrNiTi18-9, (B) X10CrMoVNb9-1, (C) 13CrMoV42, (D) X8CrNiNb16-13.
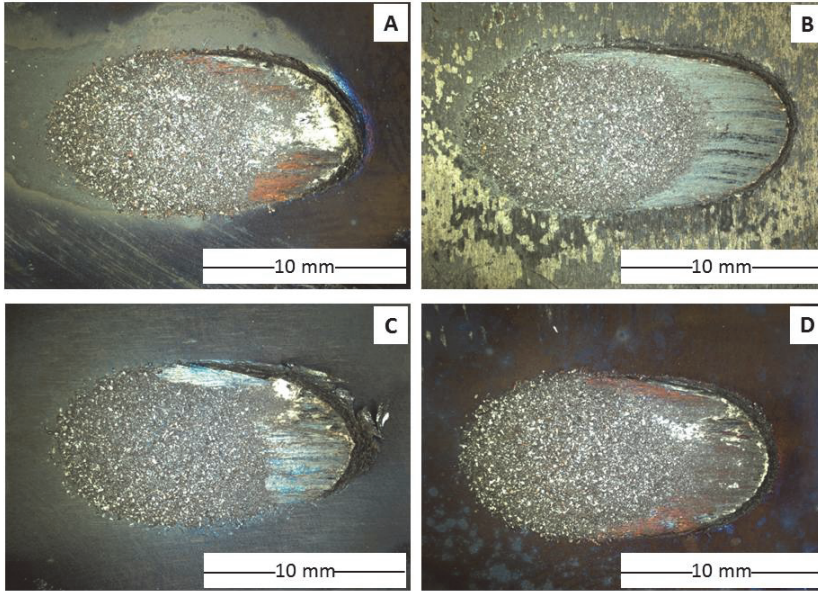
Figure 3.10. Macro images of typical wear scar of steel tested at 600 °C temperature: (A) X12CrNiTi18-9, (B) X10CrMoVNb9-1, (C) 13CrMoV42, (D) X8CrNiNb16-13.
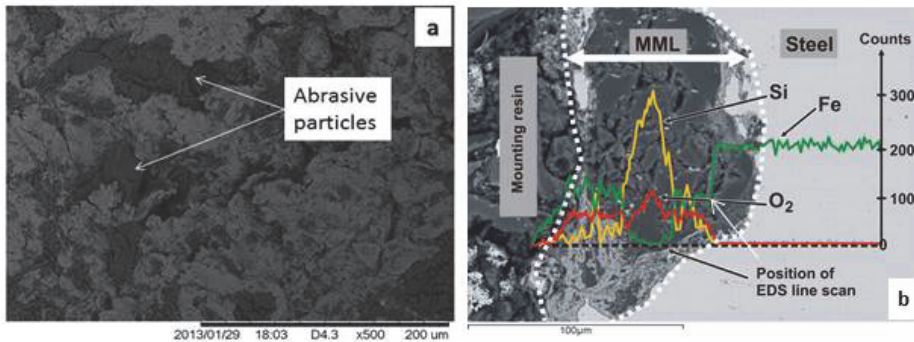
Figure 3.11. SEM micrographs of typical worn surfaces of steel B (martensitic steel X10CrMoVNb9-1) after cyclic impact/abrasion testing at 600 °C: (a) Impact zone; (b) Formation of mechanically mixed layer (MML) [PAPER II].

Additionally, qualitative analysis were performed by confocal microscopy Leica DCM 3D for steel (A) X12CrNiTi18-9. The topography and longitudinal and transverse profile of wear dimple has been measured, see Figure 3.12.
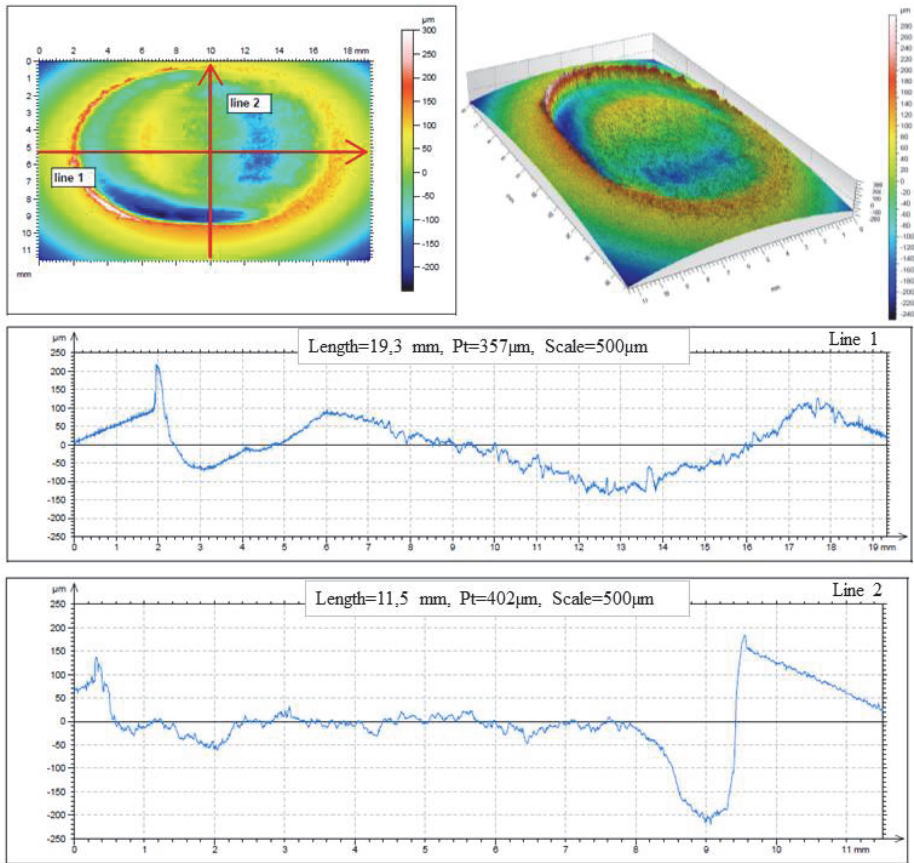
Figure 3.12. The topography and profiles of wear dimple of steel (A) X12CrNiTi18-9.

Volumetric wear maps

To summarize the volumetric wear maps (Figure 3.13, 3.14) have been proposed for the comparison of the investigated steels behaviour in different operating conditions.

TEST CONDITIONS 500°C				
EROSION, 90° [mm³/kg]	LOW 23.41	MEDIUM 25.21	HIGH 39.25	LOW 23.03
EROSION, 30° [mm³/kg]	MEDIUM 45.01	LOW 36.29	HIGH 56.50	MEDIUM 45.14
IMPACT ABRASION [mm³]	HIGH 19.62	MEDIUM 16.78	MEDIUM 14.87	LOW 11.56
GRADE	A	B	C	D
TESTED	12X18H10T	X10CrMoVNb9-1	12X1МΦ	TP347HFG
EQUIVALENT	X12CrNiTi18-9	P91	13CrMoV42	X8CrNiNb16-13

Figure 3.13. Volumetric wear map of studied steels at 500 °C.

TEST CONDITIONS 600°C				
EROSION, 90° [mm³/kg]	LOW 30.52	MEDIUM 40.72	HIGH 70.67	LOW 28.99
EROSION, 30° [mm³/kg]	LOW 40.45	MEDIUM 46.86	HIGH 74.73	MEDIUM 47.80
IMPACT ABRASION [mm³]	HIGH 23.87	MEDIUM 18.94	LOW 11.59	HIGH 21.30
GRADE	A	B	C	D
TESTED	12X18H10T	X10CrMoVNb9-1	12X1МΦ	TP347HFG
EQUIVALENT	X12CrNiTi18-9	P91	13CrMoV42	X8CrNiNb16-13

Figure 3.14. Volumetric wear map of studied steels at 600 °C.

4   GENERAL CONCLUSIONS

The corrosion, erosion and impact-abrasion of four boiler steels have been tested at high temperatures in laboratory conditions.

On the basis of the experiments tested steel grades have been ranked as follows:

- HTC: the best corrosion resistant material is austenitic steel grade (A) X12CrNiTi18-9, then are going austenitic steel (D) X8CrNiNb16-13, pearlitic steel grade (C) 13CrMoV42 and martensitic (B) X10CrMoVNb9-1.
- Oxidation: the best resistant material is austenitic steel grade (A) X12CrNiTi18-9, then are going austenitic steel (D) X8CrNiNb16-13, martensitic (B) X10CrMoVNb9-1 and pearlitic steel grade (C) 13CrMoV42.

The results have shown that the ranking of steels according to their resistance to high temperature corrosion and oxidation does not agree with the ranking on the basis of tribotests.

In order to make reasonable selection of relevant steel grade for boiler components designed for operation in definite conditions the corrosion-oxidation and abrasive wear performance maps have been proposed. The real operation conditions of the component should be taken into account.

Scientific Novelty

Scientific novelty of the doctoral thesis includes:

- New data of four boiler steel grades resistance to high temperature corrosion and abrasive wear have been obtained.
- New methodology of high temperature corrosion (HTC) testing has been proposed and realised in newly developed HTC tester.

Future work

The thesis proposed high temperature corrosion, oxidation and two types of material wear analysis: high temperature erosion and high temperature cyclic impact-abrasion.

The major interest for future researches provides high temperature corrosion in aggressive gas and ash media. It makes interest to conduct cyclic test with the kinematical growth of the corrosion layer, to measure elements with XRD-analysis in it and to find chlorine impact on corrosion velocity in gas environment.

It would be interesting to evaluate erosion-oxidation, erosion-corrosion mechanism during the tests and to plot the EO, EC maps. These maps could help to identify the regime in which a system will be operating and determine the degree of material wastage that can be expected for a given system.

In order to make more precise life time assessment of component operated in HTC conditions in the presence of oil shale ash deposits the long term field tests are required.

The EU Framework Programme for Research and Innovation Horizon 2020 [47] will provide fellowships for individual researches, which could be considered as major source of financial support.

References

[1]   Heikinheimo, L., Lahdenperä, K., Sandlin, S. Monitoring of oxidation of metals in gas environments for energy production, *Corrosion Science*, vol.45, pp. 2143 – 2161.

[2]   Ots, A. Oil Shale Fuel Combustion, Tallinn, ISBN 9949-13-710-7, ISBN 978-9949-13-710-1, 2004.

[3]   Hutchings, I.M. Tribology. UK: Edward Arnold Press, 1992.

[4]   Uuemõis, H., Kleis., I. A critical analysis of erosioon problems which have been little studied. *Wear*, 1975, 31, pp. 359 – 373.

[5]   Wellman, R.G., Nicholls, J.R. High temperature erosion-oxidation mechanisms, maps and models. *Wear,* 2004, 256, pp. 907 – 917.

[6]   Kajda S., Harvey S.S.K., Wilusz E. Encyclopedia of Tribology. Elsevier, 1990.

[7]   Suik H., Pihu T., Konist A. Catastrophic wastage of tubes in fluidized bed boiler, *Oil Shale*, 2011, V. 28, No 1S, pp. 99 – 107.

[8]   Pihu, T., Arro, H., Prikk, A., Rootamm, R., Konist, A. Corrosion of air preheater tubes of oil shale CFB boiler. Part I. Dew point of flue gas and low-temperature corrosion. *Oil Shale*, 2009, vol. 26, No.1, pp.5 – 12.

[9]   Antonov, M., Veinthal, R., Huttunen-Saarivirta, E., Hussainova, I., Vallikivi, A., Lelis, M., Priss, J. Effect of oxidation on erosive wear behaviour of boiler steels. *Tribo-Corrosion,* 2013, 68, pp. 35 – 44.

[10] Plamus, K., Ots, A., Pihu, T., Neshumayev, D. Firing Estonian oil shale in CFB boilers- ash balance and behavior of carbonate minerals. *Oil Shale*, 2011, vol. 28, No.1, pp.58 – 67.

[11] Neshumayev, D., Ots, A., Parve, T., Pihu, T., Plamus, K., Prikk, A. Combustion of Baltic oil shales in boilers with fluidized bed combustion. *Power technology and Engineering*, 2011, Vol.44, No.5.

[12] H.Suik, T.Pihu, A.Molodtsov, "Wear of the fuel supply system of CFB boilers," *Oil Shale*, 2008, vol. 25, No.2, pp.209 – 216.

[13] Adamiec, J. High temperature corrosion of power boiler components cladded with nickel alloys. *Material Characterization,* 2009, 60(10), pp.1093 – 1099.

[14] Klevtsov I., Tallermo H., Bojarinova T. Influence of Nickel and Chromium Contents on Boiler Steel High-Temperature Corrosion Resistance. *Conditions and Life Management for Power Plants – Baltica V*, 2001, Vol. I, Espoo, Finland, pp. 235 – 246.

[15] Kawahara, Y. *Corros. Sci.*, 2002, 44, pp. 223 – 245.

[16] Stack, M.M., Stott, F.H. *Corrosion Sci.*,1995, 180, 91.

[17] Wellman, R.G., Nicholls, J.R. High temperature erosion-oxidation mechanisms, maps and models. *Wear*, 2004, 256, pp. 907 – 917.

[18] Antonov, M., Hussainova, I. Experimental setup for testing and mapping of high temperature abrasion and oxidation synergy. *Wear, 2009,* 267, pp.1798 – 1803.

[19] Huttunen-Saarivirta, E., Antonov, M., Venthal, R., Tuiremo, J., Mäkelä, K., Siitonen, P. Influence of the particle impact conditions and temperature on erosion-oxidation of steels at elevated temperatures. *Wear,* 2011, 272, pp.159 – 175.

[20] Stack, M.M., Stott, F.H. *Corrosion Sci.*, 1993, 35, pp.1027

[21] Sundström, A., Rendon, J., Olsson, M. Wear behaviour of some low alloyed steels under combined impact/abrasion contact conditions. *Wear*, 2001, 250, pp. 744 – 754.

[22] James J. Dillon, Paul B. Desch, Tammy S. Lai, Daniels J. Flynn. The Nalco guide to boiler failure analysis. ISBN:0071743006, ISBN-13:9780071743006, Mcgraw-hill Professional Publishing, 2011.

[23] Badisch, E., Winkelmann, H., Franek, F. High-temperature cyclic impact abrasion testing: wear behaviour of single and multiphase materials up ti 750 °C. *Estonian Journal of Engineering,* 2009,15,4, pp. 359 – 366.

[24] Badisch, E., Katsich, C., Winkelmann, H., Franek, F., Roy, M. Wear behavior of hardfaced Fe-Cr-C alloy and austenitic steel under 2-body and 3-body conditions at elevated temperature. *Tribology International,* 2010, 43, pp.1234 – 1244.

[25] Kirchgabner, M., Badisch, E., Franek, F. Behaviour of iron-based hardfacing alloys under abrasion and impact. *Wear,* 2008, 265, pp.772 – 779.

[26] Antonov, M., Michalczewski, R., Pasaribu, R., Piekoszewski, W. Comparison of tribological model and real component test methods for lubricated contacts. *Estonian Journal of Engineering,* 2009, 15, pp. 349 – 358.

[27] RTM 108.030.116-78 Standards for Determination of Corrosive Resistance of Boiler Alloys at Elevated Temperatures (in Russian).

[28] OST 108.030.01-75 Steam Boilers. Method of Corrosion Tests, Moscow, 1973 (in Russian).

[29] Dedov, A. Assesment of Metal Condition and Remaining Life of In-service Power Plant Components Operating at High Temperature. ISSN 1406-4758, ISBN 978-9985-59-747-7, 2007.

[30] Antikain P. Corrosion of Steam Generator Metals. Energia, Moscow, 1977 (in Russian).

[31] Tallermo, H., Tomann, E., Klevtsov, I., Bojarinova, T., Nuutre, M. *Oil Shale*, 1997, 14, pp. 317 – 327.

[32] Tallermo, H., Klevtsov, I., Bojarinova, T., Dedov, A. *Oil Shale,* 2005, 22, pp. 467 – 474.

[33] Tallermo, H., Lausmaa, T., Klevtsov, I., Bojarinova, T., Dedov, A. *Oil Shale,* 1997, 14, pp. 307 – 316.

[34] Laid, J., Lootus, H., Randmann, R., Suik, H., Tallermo, H., Tomann, E., Touart, R. The study of heat resistance boiler steel grades in environment of mazut and Estonian oil shale combustion gases. Report of Thermal Engineering Department of Tallinn University of Technology, 1975, p.170.

[35] Bose, S., High Temperature Coatings, Butterworth-Heinemann, Oxford, 2007.

[36] Kim, J.K., Kim, Y.H., Lee, J.S., Kim, K.Y. *Corros. Sci*., 2010, 52, pp. 1847 – 1852.

[37] Ilevbare, G.O., Burstein, G.T. *Corros. Sci.*, 2001, 43, pp. 485 – 513.

[38] Wanklyn, J.N. *Corros. Sci.*, 1981, 21, pp. 211 – 225.

[39] Nam, N.D., Kim, J.G. *Corros. Sci.*, 2010, 52, pp. 3377 – 3384.

[40] Kleis I., Kulu P. Solid Particle Erosion. TUT Press, 2005.

[41] Winkelmann, H., Badisch, E., Kirchgaßner, M., Danninger, H. Wear mechanisms at high temperature. Part 1: Wear mechanisms of different Fe-based alloys, *Tribol. Lett*., 2009, 34, pp. 155 – 166.

[42] ISO 8407:2009(E). Corrosion of metals and alloys- Removal of corrosion products from corrosion test specimens.

[43] RTM 108.030.116–78. Method for determination of characteristics of high temperature corrosion resistance of boiler steels (in Russian).

[44] Tallermo H., Klevtsov I., Uus M. and Crane R.A. High Temperature Corrosion of Martensite Alloy Under Oil Shale Fly Ash. *ASME Journal of Pressure Vessel Technology*, 2001, Vol. 123, Issue 3, pp. 387 – 390.

[45] Rojacz, H., Zikin, A., Mozelt, C., Winkelmann, H., Badisch, *E. Surf. And Coat. Technol*., 2013, 222, pp. 90 – 96.

[46] Priss, J., Klevtsov, I., Dedov, A., Antonov, M. Erosion wear testing of boiler steels at elevated temperatures. *Proceeding of the 14th International Symposium „Topical Problems in the Field of Electrical and Power Engineering"* Pärnu, Estonia, January 13 – 17, 2014, pp. 248 – 250.

[47] European Commission. The EU Framework Programme for Research and Innovation. Project: "Horizon 2020". Available from [WWW]: http://ec.europa.eu/programmes/horizon2020/en/h2020-section/marie-sk %C5 %82odowska-curie-actions (03.02.2014)

Abstract

Investigation of Corrosion and Wear of Boiler Steels at Elevated Temperatures

Thesis is focused on the boiler steels investigation under corrosion, erosion and abrasion impact on the basis of laboratory tests. In order to analyze the boiler steels with relation to corrosion and wear at elevated temperatures the number of experiments has been performed.

High temperature corrosion tests have been carried out in AC^{2}T laboratory using new testing technique proposed by the author of the given thesis. According to this technique the HTC tests have been carried out in the media of gaseous HCl and oil shale ash. Some of the tested steel grades have been previously tested in DTE TUT using another technique namely the tests have been performed in the media of natural gas combustion products and periodically renewable oil shale ash.

The comparative analysis of HTC experimental results has shown that the results of HTC experiments, which have been carried out in laboratory of AC^{2}T are in a good agreement with results obtained from the tests conducted in DTE TUT for three investigated steels. Thus a good agreement of the results allows to consider used in AC^{2}T technique for HTC investigation as a valid one and the results to be reliable. Moreover the AC^{2}T technique has an advantage in comparison with DTE TUT technique because it does not require periodical interrupting of the experiment for oil shale ash renewal.

HTC tests of investigated boiler steel grades in the presence of sulphur and potassium containing oil shale ash have shown that the best corrosion resistant is austenitic steel grade (A) X12CrNiTi18-9, then are going austenitic steel (D) X8CrNiNb16-13, pearlitic steel grade (C) 13CrMoV42 and martensitic (B) X10CrMoVNb9-1. That sequence represents the corrosion ranking of the tested steel grades for their application as high-temperature heating surfaces in boilers firing oil shale which contain chlorine, sulphur and potassium in outer deposits.

Obtained ranking and HTC tests results could be used for selection of steel for boiler components designed for operation in similar conditions. Right steel selection could help to increase the durability and operating reliability of boiler components.

The oxidation rate of the steels in high temperature oxidative environment (air) was also investigated and the ranking of steel grades resistance in these conditions was as follows: the best resistant is austenitic steel grade (A) X12CrNiTi18-9, then are going austenitic steel (D) X8CrNiNb16-13, martensitic (B) X10CrMoVNb9-1 and pearlitic steel grade (C) 13CrMoV42.

Solid particle erosion tests have been performed in TUT laboratory. The abrasive particles used in this work were rounded silica particles. Investigation of steady state erosion rate was made as a function of the impact angle. Erosion tests were conducted at impact angles of 30° and 90°. It was found that the best high temperature erosion resistance shows austenitic steel grade (A)

X12CrNiTi18-9, then are going austenitic steel (D) X8CrNiNb16-13, martensitic (B) X10CrMoVNb9-1 and pearlitic steel grade (C) 13CrMoV42.The volumetric wear rate of the steels B, C and D increases with temperature increasing. Opposite behaviour can be detected for austenitic steel A which exhibits better wear performance at higher testing temperature of 600 °C in test with impact angle of abrasive 30°. That may be explained by particle sticking. It was also found that the volumetric wear rate is lower with impact angle of 90°.

All of investigated steels have been subjected to high-temperature cyclic impact abrasion testing as well. The tests have been performed in AC²T laboratory. The specimens were fixed at 45° and periodically hit by the plunger at 1.8-2.0 Hz frequency with a constant flow of abrasive. Tests have been carried out at the temperatures 500 °C and 600 °C. The characterization of wear behaviour has been done by determining the weight loss.

It was found that the best wear resistance shows pearlitic steel grade (C) 13CrMoV42.The volumetric wear rate of the steels A, B, and D increases with temperature increase. Opposite behaviour can be detected for pearlitic steel grade (C) which exhibits better wear resistance at higher testing temperature of 600 °C. It could be explained by the sticking of the abrasive particles to the specimen surface that decreases the rate of steel wear. This conclusion has been made on the basis of SEM analysis of the tested specimen surface.

The results of carried out investigations of boiler steels X12CrNiTi18-9, X10CrMoVNb9-1, 13CrMoV42 and X8CrNiNb16-13have shown that the ranking of steels according to their resistance to high temperature corrosion and oxidation does not agree with the ranking on the basis of tribotests. Thus in order to select relevant steel grade for particular boiler component the real operation conditions of the component should be taken into account. To summarize the corrosion-oxidation-wear rate maps have been proposed for the comparison of the investigated steels behaviour in different operating conditions.

Kokkuvõte

Katlateraste kõrgetemperatuurilise korrosiooni- ja kulumisuuringud

Väitekiri on keskendunud katlamaterjalide korrosiooni, erosiooni ja abrasiooni laboratoorsetele uuringutele. Katlamaterjalide korrosiooni ja kulumise uurimiseks kõrgetel temperatuuridel tehti rida katseid.

Kõrgetemperatuurilise korrosiooni katsed viidi läbi AC^2T laboratooriumis kasutades uut, antud väitekirja autori poolt väljamõeldud katsemeetodit. Vastavalt sellele meetodile tehti kõrgetemperatuurilise korrosiooni katsed gaasilise HCl ja põlevkivi tuha keskkonnas. Mõningaid katsetatud terasemarke oli varem katsetatud TTÜ STI-s kasutades teist meetodit, nimelt tehti katsed loodusliku gaasi põlemissaaduste keskkonnas ja perioodiliselt uuendatava põlevkivi tuhaga.

Kõrgetemperatuurilise korrosioonikatsete tulemuste võrdlus näitas, et kolmele terasemargile AC^2T laboratooriumis saadud tulemused on heas kooskõlas varem TTÜ STI-s saadud tulemustega. Tulemuste hea kokkulangevus näitab, et AC^2T-s kasutatud meetod toimib ja on usaldusväärne. Veelgi enam, AC^2T-s kasutatud meetodil on TTÜ STI meetodi ees mõningane eelis, sest puudub vajadus katkestada katse põlevkivi tuha uuendamiseks.

Katlateraste kõrgetemperatuurilised katsed väävlit ja kaaliumit sisaldava põlevkivi tuha juuresolekul on näidanud, et kõige suurem vastupanu korrosioonile on austeniitterasel (A) X12CrNiTi18-9. Talle järgnevad korrosioonikindluse kahanevas järjekorras austeniitteras (D) X8CrNiNb16-13, perliitteras (C) 13CrMoV42 ja martensiitteras (B) X10CrMoVNb9-1. See järjestus annab katsetatud teraste reastuse nende kasutamisel kõrgetemperatuurilistes küttepindades põlevkivi põletamisel, kus gaasipoolsed sadestused sisaldavad kloori, väävlit ja kaaliumit.

Saadud katlateraste järjestust ja kõrgetemperatuuriliste korrosioonikatsete tulemusi saab kasutada sarnastes tingimustes töötavate katlakomponentide materjalide valikuks. Materjalide õige valik aitab tõsta katlakomponentide tööiga ja töökindlust.

Samuti uuriti materjalide korrosioonikindlust kõrgetemperatuurilises oksüdeerivas keskkonnas (õhk) ja saadud korrosioonikindluse järjestus on järgmine: parim on austeniitteras (A) X12CrNiTi18-9, millele järgnevad austeniitteras (D) X8CrNiNb16-13, martensiitteras (B) X10CrMoVNb9-1 ja perliitteras (C) 13CrMoV42.

Tahkete osakeste erosioonikatsed tehti TTÜ laboris, kasutades abrasiivsete osakestena ümmargusi räniosakesi. Statsionaarset erosioonikiirust uuriti lööginurga funktsioonina, valides lööginurkadeks 30° ja 90°. Leiti, et suurimat vastupanu kõrgetemperatuurilisele erosioonile osutab auteniitteras (A) X12CrNiTi18-9, millele järgnevad austeniitteras (D) X8CrNiNb16-13, martensiitteras (B) X10CrMoVNb9-1 ja perliitteras (C) 13CrMoV42. Materjalide B, C, ja D mahuline kulumine suureneb temperatuuri tõusuga.

Vastupidist käitumist võib täheldada austeniitterase A korral, mis näitab paremat kulumiskindlust kõrgemal temperatuuril 600 °C juures 30° lööginurga korral. Seda võib seletada osakeste kleepuvusega. Ühtlasi tuvastati, et 90°-se lööginurga korral on mahulise kulumise kiirus väiksem.

Kõiki uuritud materjale katsetati ka kõrgel temperatuuril tsüklilise abrasiooni tingimustes. Katsed viidi läbi AC^2T laboratooriumis. 45°-se nurga all kinnitatud katsekehi pommitati sagedusega 1,8÷2,0 Hz konstantse abrasiivmaterjali joaga. Katsed viidi läbi temperatuuridel 500 °C ja 600 °C. Kulumise iseloomu määrati kaalukao järgi.

Tuvastati, et parimat kulumiskindlust näitas perliitteras (C) 13CrMoV42. Materjalide A, B ja D mahulise kulumine suureneb temperatuuri tõusuga. Vastupidiselt käitub perliitteras C, mis näitab suuremat kulumiskindlust kõrgemal temperatuuril 600 °C juures. Seda võib seletada abrasiivosakeste kleepumisega katsekeha pinnale, mis vähendab sel viisil kulumise kiirust. Selline järeldus tehti katsekehade pinna skaneeriva elektronmikroskoobiga analüüsimise tulemusel.

Katlaterastega X12CrNiTi18-9, X10CrMoVNb9-1, 13CrMoV42 ja X8CrNiNb16-13 läbiviidud uuringud näitasid, et nende järjestus kõrgetemperatuurilise korrosiooni- ja oksüdeerumiskindluse järgi ei lange kokku nende järjestusega tsüklilise kulumiskindluse järgi. Seega tuleb igale katla-komponendile sobiva terasemargi valikul võtta arvesse tegelikke töötingimusi. Uuritud katlateraste korrosiooni-oksüdeerimis-kulumiskindlusest täieliku ülevaate saamiseks pannakse töös ette võrrelda nende materjalide käitumist erinevates töötingimustes.

Elulookirjeldus

Isikuandmed

Ees- ja perekonnanimi	Jelena Priss
Sünniaeg ja -koht	16.05.1983, Eesti
Kodakondsus	Eesti
E-posti aadress	jelenapriss@gmail.com

1. *Hariduskäik*

Õppeasutus	Lõpetamise aeg	Haridus (eriala/kraad)
Pärnu Vene Gümnaasium	2002	Keskkool
Tallinna Tehnikaülikool (TTÜ)	2005	Bakalaureusekraad, Soojustehnika
Tallinna Tehnikaülikool (TTÜ)	2007	Magistrikraad, Soojustehnika
Tallinna Tehnikaülikool (TTÜ)	2014	Doktoriõpe, Soojustehnika

2. *Keelteoskus (alg-, kesk- või kõrgtase)*

Keel	Tase
Vene	Emakeel
Eesti	Kõrgtase
Inglise	Kesktase

3. *Täiendusõpe*

Õppimise aeg	Täiendusõppe korraldaja nimetus
2008- Koolitus „Training Programme on Renewable Energy and Energy Efficiency" (18 päeva)	The Energy and Resources Institute, New Delhi, India
2011- 10th International Symposium „Topical Problems in the Field of Electrical and Power Engineering" (5 days)	Doctoral School of Energy and Geotechnology, Pärnu, Estonia.

2012- 11th International Symposium „Topical Problems in the Field of Electrical and Power Engineering" (5 days)	Doctoral School of Energy and Geotechnology, Pärnu, Estonia.
2012- 12th International Symposium „Topical Problems in the Field of Electrical and Power Engineering" (5 days)	Doctoral School of Energy and Geotechnology, Kuressaare, Estonia.
2012- Välisõppe 5 kuud	AC^{2}T, Wiener Neustadt, Austria
2014- 14th International Symposium „Topical Problems in the Field of Electrical and Power Engineering" (5 days)	Doctoral School of Energy and Geotechnology, Pärnu, Estonia.

4. *Teenistuskäik*

Töötamise aeg	Tööandja nimetus	Ametikoht
2004	Tallinna Kütte AS	Praktikant
2006 – 2008	Projektide Agentuur OÜ	Tehniline joonistaja
2008 – 2012	Sweco Project AS	Tööstusosakond, insener
2012	AC^{2}T, Austria	Teadur
2012 – 2014	Sweco Project AS	Tööstusosakond, insener

5. *Teadustegevus*

- **Priss J.,** Rojacz H., Klevtsov I., Dedov A., Winkelmann H., Badisch E. High temperature corrosion of boiler steels in hydrochloric atmosphere under oil shale ashes. *Corrosion Science*, 2014, 82, pp. 36–44. DOI: http://dx.doi.org/10.1016/j.corsci.2013.12.016

- **Priss J**., Klevtsov I., Dedov A., Antonov M., Rojacz H., Badisch E. High temperature cyclic impact/abrasion testing of boiler steels. *Key Engineering Materials,* 2014, 604, pp. 289–292. DOI: 10.4028/www.scientific.net/KEM.604.289

- Antonov M., Veinthal R., Huttunen-Saarivirta E., Hussainova I., Vallikivi A., Lelis M., **Priss J**. Effect of oxidation on erosive wear behaviour of boiler steels. *Tribo-Corrosion*, 2013, 68, pp. 35–44. Elsevier. DOI: http://dx.doi.org/10.1016/j.triboint.2012.09.011
- **Priss J**., Klevtsov I., Dedov A., Antonov M. Investigation of boiler materials in respect to corrosion and wear. *"Proceedings of the 9th DAAAM Baltic Conference"* 24–26th April 2014, Tallinn, Estonia.
- **Priss J.**, Klevtsov I. Strength calculations of slurry disposal pipeline. *Proceedings of the 22nd DAAAM World Symposium*. 23–26th November 2011, Austria Center Vienna, Vienna, Austria, pp. 1175–1176.
- **Priss J.**, Klevtsov I., Winkelmann H. High–temperature chlorine corrosion in presence of sulphur-containing and potassium external deposits. *Proceeding of the 23rd International DAAAM Symposium*. 24-27th of October, 2012, Zadar, Croatia. Volume 23, No.1, ISSN 2304–1382, pp. 0911 – 0916.
- **Priss J.**, Klevtsov I., Dedov A., Antonov M. Investigation of boiler materials in respect to corrosion and wear. *"Proceedings of the 9th DAAAM Baltic Conference"* 24–26th April 2014, Tallinn, Estonia.

Curriculum Vitae

Personal data

Name	Jelena Priss
Date and place of birth	16.05.1983, Estonia
E-mail	jelenapriss@gmail.com

1. Education

Education Institution	Graduation year	Education (field of study/degree)
Pärnu Russian Gymnasium	2002	Secondary Education
Tallinn University of Technology (TUT)	2005	B. Sc., Thermal Engineering
Tallinn University of Technology (TUT)	2007	M. Sc., Thermal Engineering
Tallinn University of Technology (TUT)	2014	Ph.D. studies, Thermal Engineering

2. Language competence/skills (fluent, average, Basic skills)

Language	Level
Russian	Mother tongue
Estonian	Fluent
English	Average

3. Special courses

Period	Educational or other organisation
2008- Training Programme on Renewable Energy and Energy Efficiency (18 days)	The Energy and Resources Institute, New Delhi, India
2011- 10th International Symposium „Topical Problems in the Field of Electrical and Power Engineering" (5 days)	Doctoral School of Energy and Geotechnology, Pärnu, Estonia.

2012- 11th International Symposium „Topical Problems in the Field of Electrical and Power Engineering" (5 days)	Doctoral School of Energy and Geotechnology, Pärnu, Estonia.
2012- 12th International Symposium „Topical Problems in the Field of Electrical and Power Engineering" (5 days)	Doctoral School of Energy and Geotechnology, Kuressaare, Estonia.
2012- Traineeship as a guest scientist (5 months)	AC^{2}T, Wiener Neustadt, Austria
2014- 14th International Symposium „Topical Problems in the Field of Electrical and Power Engineering" (5 days)	Doctoral School of Energy and Geotechnology, Pärnu, Estonia.

4. Professional employment

Period	Organisation	Position
2004	Tallinna Kütte AS	Training
2006 – 2008	Projektide Agentuur OÜ	Technical designer
2008 – 2012	Sweco Project AS	Industrial department, Engineer
2012	AC^{2}T, Austria	Traineeship as a guest scientist
2012 – 2014	Sweco Project AS	Industrial department, Engineer

5. Scientific work

- **Priss J.,** Rojacz H., Klevtsov I., Dedov A., Winkelmann H., Badisch E. High temperature corrosion of boiler steels in hydrochloric atmosphere under oil shale ashes. *Corrosion Science*, 2014, 82, pp. 36–44. DOI: http://dx.doi.org/10.1016/j.corsci.2013.12.016

- **Priss J**., Klevtsov I., Dedov A., Antonov M., Rojacz H., Badisch E. High temperature cyclic impact/abrasion testing of boiler steels. *Key Engineering Materials,* 2014, 604, pp. 289–292. DOI: 10.4028/www.scientific.net/KEM.604.289

- Antonov M., Veinthal R., Huttunen-Saarivirta E., Hussainova I., Vallikivi A., Lelis M., **Priss J**. Effect of oxidation on erosive wear behaviour of boiler steels. *Tribo-Corrosion*, 2013, 68, pp. 35–44. Elsevier. DOI: http://dx.doi.org/10.1016/j.triboint.2012.09.011
- **Priss J**., Klevtsov I., Dedov A., Antonov M. Investigation of boiler materials in respect to corrosion and wear. *"Proceedings of the 9th DAAAM Baltic Conference"* 24–26th April 2014, Tallinn, Estonia.
- **Priss J.**, Klevtsov I. Strength calculations of slurry disposal pipeline. *Proceedings of the 22nd DAAAM World Symposium*. 23–26th November 2011, Austria Center Vienna, Vienna, Austria, pp. 1175–1176.
- **Priss J.**, Klevtsov I., Winkelmann H. High–temperature chlorine corrosion in presence of sulphur-containing and potassium external deposits. *Proceeding of the 23rd International DAAAM Symposium.* 24-27th of October, 2012, Zadar, Croatia. Volume 23, No.1, ISSN 2304–1382, pp. 0911 – 0916.
- **Priss J.**, Klevtsov I., Dedov A., Antonov M. Investigation of boiler materials in respect to corrosion and wear. *"Proceedings of the 9th DAAAM Baltic Conference"* 24–26th April 2014, Tallinn, Estonia.

DISSERTATIONS DEFENDED AT
TALLINN UNIVERSITY OF TECHNOLOGY ON
MECHANICAL ENGINEERING

1. **Jakob Kübarsepp**. Steel-Bonded Hardmetals. 1992.

2. **Jakub Kõo**. Determination of Residual Stresses in Coatings &Coated Parts. 1994.

3. **Mart Tamre**. Tribocharacteristics of Journal Bearings Unlocated Axis. 1995.

4. **Paul Kallas**. Abrasive Erosion of Powder Materials. 1996.

5. **Jüri Pirso**. Titanium and Chromium Carbide Based Cermets. 1996.

6. **Heinrich Reshetnyak**. Hard Metals Serviceability in Sheet Metal Forming Operations. 1996.

7. **Arvi Kruusing**. Magnetic Microdevices and Their Fabrication methods. 1997.

8. **Roberto Carmona Davila**. Some Contributions to the Quality Control in Motor Car Industry. 1999.

9. **Harri Annuka**. Characterization and Application of TiC-Based Iron Alloys Bonded Cermets. 1999.

10. **Irina Hussainova**. Investigation of Particle-Wall Collision and Erosion Prediction. 1999.

11. **Edi Kulderknup**. Reliability and Uncertainty of Quality Measurement. 2000.

12. **Vitali Podgurski**. Laser Ablation and Thermal Evaporation of Thin Films and Structures. 2001.

13. **Igor Penkov**. Strength Investigation of Threaded Joints Under Static and Dynamic Loading. 2001.

14. **Martin Eerme**. Structural Modelling of Engineering Products and Realisation of Computer-Based Environment for Product Development. 2001.

15. **Toivo Tähemaa**. Assurance of Synergy and Competitive Dependability at Non-Safety-Critical Mechatronics Systems design. 2002.

16. **Jüri Resev**. Virtual Differential as Torque Distribution Control Unit in Automotive Propulsion Systems. 2002.

17. **Toomas Pihl**. Powder Coatings for Abrasive Wear. 2002.

18. **Sergei Letunovitš**. Tribology of Fine-Grained Cermets. 2003.

19. **Tatyana Karaulova**. Development of the Modelling Tool for the Analysis of the Production Process and its Entities for the SME. 2004.

20. **Grigori Nekrassov**. Development of an Intelligent Integrated Environment for Computer. 2004.

21. **Sergei Zimakov**. Novel Wear Resistant WC-Based Thermal Sprayed Coatings. 2004.

22. **Irina Preis**. Fatigue Performance and Mechanical Reliability of Cemented Carbides. 2004.

23. **Medhat Hussainov**. Effect of Solid Particles on Turbulence of Gas in Two-Phase Flows. 2005.

24. **Frid Kaljas**. Synergy-Based Approach to Design of the Interdisciplinary Systems. 2005.

25. **Dmitri Neshumayev**. Experimental and Numerical Investigation of Combined Heat Transfer Enhancement Technique in Gas-Heated Channels. 2005.

26. **Renno Veinthal**. Characterization and Modelling of Erosion Wear of Powder Composite Materials and Coatings. 2005.

27. **Sergei Tisler**. Deposition of Solid Particles from Aerosol Flow in Laminar Flat-Plate Boundary Layer. 2006.

28. **Tauno Otto**. Models for Monitoring of Technological Processes and Production Systems. 2006.

29. **Maksim Antonov**. Assessment of Cermets Performance in Aggressive Media. 2006.

30. **Tatjana Barashkova**. Research of the Effect of Correlation at the Measurement of Alternating Voltage. 2006.

31. **Jaan Kers**. Recycling of Composite Plastics. 2006.

32. **Raivo Sell**. Model Based Mechatronic Systems Modeling Methodology in Conceptual Design Stage. 2007.

33. **Hans Rämmal**. Experimental Methods for Sound Propagation Studies in Automotive Duct Systems. 2007.

34. **Meelis Pohlak**. Rapid Prototyping of Sheet Metal Components with Incremental Sheet Forming Technology. 2007.

35. **Priidu Peetsalu**. Microstructural Aspects of Thermal Sprayed WC-Co Coatings and Ni-Cr Coated Steels. 2007.

36. **Lauri Kollo**. Sinter/HIP Technology of TiC-Based Cermets. 2007.

37. **Andrei Dedov**. Assessment of Metal Condition and Remaining Life of In-service Power Plant Components Operating at High Temperature. 2007.

38. **Fjodor Sergejev**. Investigation of the Fatigue Mechanics Aspects of PM Hardmetals and Cermets. 2007.

39. **Eduard Ševtšenko**. Intelligent Decision Support System for the Network of Collaborative SME-s. 2007.

40. **Rünno Lumiste**. Networks and Innovation in Machinery and Electronics Industry and Enterprises (Estonian Case Studies). 2008.

41. **Kristo Karjust**. Integrated Product Development and Production Technology of Large Composite Plastic Products. 2008.

42. **Mart Saarna**. Fatigue Characteristics of PM Steels. 2008.

43. **Eduard Kimmari**. Exothermically Synthesized B_4C-Al Composites for Dry Sliding. 2008.

44. **Indrek Abiline**. Calibration Methods of Coating Thickness Gauges. 2008.

45. **Tiit Hindreus**. Synergy-Based Approach to Quality Assurance. 2009.

46. **Karl Raba**. Uncertainty Focused Product Improvement Models. 2009.

47. **Riho Tarbe**. Abrasive Impact Wear: Tester, Wear and Grindability Studies. 2009.

48. **Kristjan Juhani**. Reactive Sintered Chromium and Titanium Carbide-Based Cermets. 2009.

49. **Nadežda Dementjeva**. Energy Planning Model Analysis and Their Adaptability for Estonian Energy Sector. 2009.

50. **Igor Krupenski**. Numerical Simulation of Two-Phase Turbulent Flows in Ash Circulating Fluidized Bed. 2010.

51. **Aleksandr Hlebnikov**. The Analysis of Efficiency and Optimization of District Heating Networks in Estonia. 2010.

52. **Andres Petritšenko**. Vibration of Ladder Frames. 2010.

53. **Renee Joost**. Novel Methods for Hardmetal Production and Recycling. 2010.

54. **Andre Gregor**. Hard PVD Coatings for Tooling. 2010.

55. **Tõnu Roosaar**. Wear Performance of WC- and TiC-Based Ceramic-Metallic Composites. 2010.

56. **Alina Sivitski**. Sliding Wear of PVD Hard Coatings: Fatigue and Measurement Aspects. 2010.

57. **Sergei Kramanenko**. Fractal Approach for Multiple Project Management in Manufacturing Enterprises. 2010.

58. **Eduard Latõsov**. Model for the Analysis of Combined Heat and Power Production. 2011.

59. **Jürgen Riim**. Calibration Methods of Coating Thickness Standards. 2011.

60. **Andrei Surzhenkov**. Duplex Treatment of Steel Surface. 2011.

61. **Steffen Dahms**. Diffusion Welding of Different Materials. 2011.

62. **Birthe Matsi**. Research of Innovation Capasity Monitoring Methodology for Engineering Industry. 2011.

63. **Peeter Ross**. Data Sharing and Shared Workflow in Medical Imaging. 2011.

64. **Siim Link**. Reactivity of Woody and Herbaceous Biomass Chars. 2011.

65. **Kristjan Plamus**. The Impact of Oil Shale Calorific Value on CFB Boiler Thermal Efficiency and Environment. 2012.

66. **Aleksei Tšinjan**. Performance of Tool Materials in Blanking. 2012.

67. **Martinš Sarkans**. Synergy Deployment at Early Evaluation of Modularity of the Multi-Agent Production Systems. 2012.

68. **Sven Seiler**. Laboratory as a Service – A Holistic Framework for Remote and Virtual Labs. 2012.

69. **Tarmo Velsker**. Design Optimization of Steel and Glass Structures. 2012.

70. **Madis Tiik**. Access Rights and Organizational Management in Implementation of Estonian Electronic Health Record System. 2012.

71. **Marina Kostina**. Reliability Management of Manufacturing Processes in Machinery Enterprises. 2012.

72. **Robert Hudjakov**. Long-Range Navigation for Unmanned Off-Road Ground Vehicle. 2012.

73. **Arkadi Zikin**. Advanced Multiphase Tribo-Functional PTA Hardfacings. 2013.

74. **Alar Konist**. Environmental Aspects of Oil Shale Power Production. 2013.

75. **Inge Roos**. Methodology for Calculating CO_2 Emissions from Estonian Shale Oil Industry. 2013.

76. **Dmitri Shvarts**. Global 3D Map Merging Methods for Robot Navigation. 2013.

77. **Kaia Lõun**. Company's Strategy Based Formation of e-Workplace Performance in the Engineering Industry. 2013.

78. **Maido Hiiemaa**. Motion Planner for Skid-Steer Unmanned Ground Vehicle. 2013.

79. **Dmitri Goljandin**. Disintegrator Milling System Development and Milling Technologies of Different Materials. 2013.

80. **Dmitri Aleksandrov**. Light-Weight Multicopter Structural Design for Energy Saving. 2013.

82. **Heiki Tiikoja**. Experimental Acoustic Characterization of Automotive Inlet and Exhaust System. 2014.